CrossMark

Nonlocal operators with local boundary conditions in higher dimensions

Burak Aksoylu[1,2] (iD) · Fatih Celiker[2] ·
Orsan Kilicer[3,4]

Abstract We present novel nonlocal governing operators in 2D/3D for wave propagation and diffusion. The operators are inspired by peridynamics. They agree with the original peridynamics operator in the bulk of the domain and simultaneously enforce local boundary conditions (BC). The main ingredients are periodic, antiperiodic, and mixed extensions of separable kernel functions together with even and odd parts of bivariate functions on rectangular/box domains. The operators are bounded and self-adjoint. We present all possible 36 different types of BC in 2D which include pure and mixed combinations of Neumann, Dirichlet, periodic, and antiperiodic BC. Our construction is systematic and easy to follow. We provide numerical experiments that

---

Communicated by: Ilaria Perugia

The original version of this article was revised: In the original publication, Figure 4 image should be Figure 5 and Figure 5 image was a repetition of Figure 6. The original article was updated by correcting the images of figures 4 and 5.

✉ Burak Aksoylu
burak@wayne.edu

Fatih Celiker
celiker@wayne.edu

Orsan Kilicer
okilicer@math.tamu.edu

[1]   US Army Research Laboratory, Attn:RDRL-WMM-B, Aberdeen Proving Ground, Aberdeen,
      MD 21005, USA

[2]   Department of Mathematics, Wayne State University, 656 W. Kirby, Detroit, MI 48202, USA

[3]   Department of Mathematics, Middle East Technical University, Ankara, Turkey

[4]   Present address: Department of Mathematics, Texas A&M University, College Station, TX, USA

⚛ Springer

verify our theoretical findings. We also compare the solutions of the classical wave and heat equations to their nonlocal counterparts.

Keywords Nonlocal wave propagation · Nonlocal diffusion · Nonlocal operator · Local boundary condition

Mathematics Subject Classification (2010) 35L05 · 65R99

1 Introduction

We extend our work in 1D [4] to higher dimensions. We construct novel governing operators for nonlocal wave propagation and nonlocal diffusion in 2D/3D. The operators are inspired by the theory of peridynamics, a nonlocal formulation of continuum mechanics developed by Silling [26]. By suppressing the time variable t, we define the operator

$$\mathcal{L}u(x, y) := cu(x, y) - \iint_{\Omega} \widehat{C}(x' - x, y' - y)u(x', y')dx'dy', \quad (x, y) \in \Omega, \quad (1.1)$$

where the 2D domain is $\Omega := (-1, 1) \times (-1, 1)$ and $c := \iint_{\Omega} C(x', y')dx'dy'$ with $C := \widehat{C}|_{\Omega}$. The operator used for nonlocal diffusion [11, 17] is

$$\mathcal{L}_{\text{orig}}u(x, y) := \iint_{\Omega} \widehat{C}(x' - x, y' - y)u(x, y)dx'dy'$$
$$- \iint_{\Omega} \widehat{C}(x' - x, y' - y)u(x', y')dx'dy'. \quad (1.2)$$

As the main contribution, we will prove that the two operators agree in the bulk of Ω, and that $\mathcal{L}$ enforces local pure and mixed Neumann, Dirichlet, periodic, and antiperiodic boundary conditions (BC).

Our approach to nonlocal problems is fundamentally different because we exclusively want to use local BC. In [12], one of our major results was the finding that the governing operator of peridynamics equation [26] in $\mathbb{R}$ and nonlocal diffusion in $\mathbb{R}^d$ are functions of the Laplace operator. This result opened the path to the introduction of local BC into nonlocal problems. Since $\mathcal{L}_{\text{orig}}$ is a nonlocal operator, one might expect only the appearance of nonlocal BC while employing it as the governing operator [17]. We establish that local BC are compatible with nonlocal operators. Our operators present an alternative to nonlocal BC and we hope that the ability to enforce local BC will provide a remedy for surface effects seen in peridynamics; see [21, 22].

We studied various aspects of local BC in nonlocal problems [1–5, 12]. Building on [12], we generalized the results in $\mathbb{R}$ to bounded domains [1, 2], a critical feature for all practical applications. In [2], we laid the theoretical foundations and in

[1], we applied the foundations to prominent BC such as Dirichlet and Neumann, and presented numerical implementation of the corresponding wave propagation. In [5], we present how to apply functional calculus to general nonlocal problems in a methodical way.

In [4], we constructed the first 1D operators that agree with the original bond-based peridynamics operator in the bulk of the domain and simultaneously enforce local Neumann and Dirichlet BC which we denote by $\mathcal{M}_N$ and $\mathcal{M}_D$, respectively. We carried out numerical experiments by utilizing $\mathcal{M}_N$ and $\mathcal{M}_D$ as governing operators in [1]. Similar classes of operators are used in various applications such as nonlocal diffusion [11, 17], image processing [18], population models, particle systems, phase transition, and coagulation, to name a few. See the studies dedicated to other related governing operators [3], conditioning analysis, domain decomposition and variational theory [8–10], and discretization [10, 27]. In this paper, we generalize the operators in 1D [4] to higher dimensions with separable kernel functions which lend themselves to a tensor product structure. However, the generalization of the 1D ideas and techniques to higher dimensions is nontrivial. More precisely, new multivariate projection operators have to be defined, their commutativity properties need to be discovered and exploited, new BC combinations arise in higher dimensions, which in turn require us to define new extensions of the kernel function.

Fractional diffusion and fractional PDEs also fall into the class of nonlocal problems [11, 15, 16, 24]. There is a fundamental difference between these operators and ours: Our governing operators are bounded. See [12, Lemma 5 and Thm. 6] and [2, Cor. 2 and Thm. 4]. Since our ultimate goal is to capture discontinuities or cracks, we are mainly interested in bounded governing operators. Fractional operators become unbounded for such discontinuities, and hence, we exclude them from our discussion.

The rest of the paper is structured as follows. In Section 2, first we prove that the operators $\mathcal{L}_{\text{orig}}$ and $\mathcal{L}$ agree in the bulk in 2D. We define the novel operators using orthogonal projections on bivariate functions for which we utilize the periodic, antiperiodic, and mixed extensions of the kernel function $C(x)$. We give the main theorem in 2D. In Section 3, first we prove that the novel operators are self-adjoint. We quote the earlier results from [4] and construct additional operators. In Section 4, we exploit the properties of the operators in 1D to construct the novel operators in 2D. We transfer the agreement in the bulk property established for univariate functions to bivariate ones and eventually prove that the novel operators agree with $\mathcal{L}_{\text{orig}}$ in the bulk in 2D. In Section 5, we make use of the Leibniz Rule, the Fubini, and the Lebesgue Dominated Convergence Theorems to prove that the novel operators enforce the local BC stated in the main theorem. In Section 6, we present all possible 36 types of BC in 2D. We provide the recipe for each possible BC in the form of a table. In Section 7, we present the operators in 3D which can be easily extended to arbitrary dimension. In Section 8, we report the numerical experiments in which we demonstrate that the prescribed BC are indeed satisfied. We also carry out a comparison of the solutions to the classical wave and heat equations to those of nonlocal ones. We conclude in Section 9.

2 The novel operators in 2D

For $(x, y), (x', y') \in \Omega$, it follows that $(x' - x, y' - y) \in (-2, 2) \times (-2, 2)$. Hence, in (1.2), the kernel function $C(x, y)$ needs to be extended from Ω^1 to the domain of $\widehat{C}(x' - x, y' - y)$, which is $\widehat{\Omega} := (-2, 2) \times (-2, 2)$ (the domain of computation). Throughout the paper, we denote the restriction of a function $\widehat{Z} : \widehat{\Omega} \to \mathbb{R}$ to Ω as Z, i.e., $Z := \widehat{Z}|_\Omega$. Furthermore, the kernel function $C(x, y)$ is assumed to be nonnegative and even. Namely,

$$C(-x, -y) = C(x, y).$$

The important choice of $C(x, y)$ is the *canonical* kernel function $\chi_\delta(x, y)$ whose only role is the representation of the nonlocal neighborhood, called the *horizon*, by a characteristic function. More precisely, for $(x, y) \in \Omega$,

$$\chi_\delta(x, y) := \begin{cases} 1, & (x, y) \in (-\delta, \delta) \times (-\delta, \delta) \\ 0, & \text{otherwise.} \end{cases} \tag{2.1}$$

The size of nonlocality is determined by δ and we assume $\delta < 1$. Since the horizon is constructed by $\chi_\delta(x, y)$, a kernel function used in practice is in the form

$$C(x, y) = \chi_\delta(x, y)\mu(x, y),$$

where $\mu(x, y) \in L^2(\Omega)$ is even.

Throughout the paper, we assume that

$$u(x, y) \in L^2(\Omega). \tag{2.2}$$

Inspired by the projections that give the even and odd parts of a univariate function, we define the following operators that act on a bivariate function.

$$P_{e,x'}, P_{o,x'}, P_{e,y'}, P_{o,y'} : L^2(\Omega) \to L^2(\Omega),$$

whose definitions are

$$P_{e,x'}u(x', y') := \frac{u(x', y') + u(-x', y')}{2}, \quad P_{o,x'}u(x', y') := \frac{u(x', y') - u(-x', y')}{2}, \tag{2.3}$$

$$P_{e,y'}u(x', y') := \frac{u(x', y') + u(x', -y')}{2}, \quad P_{o,y'}u(x', y') := \frac{u(x', y') - u(x', -y')}{2}. \tag{2.4}$$

Each operator is an orthogonal projection and possesses the following decomposition property

$$P_{e,x'} + P_{o,x'} = I_{x'}, \quad P_{e,y'} + P_{o,y'} = I_{y'}. \tag{2.5}$$

---

[1]We do not explicitly denote the dimension of the domain Ω. The dimension is implied by the number of iterated integrals present in the operator. The domain Ω is equal to $(-1, 1)$, $(-1, 1) \times (-1, 1)$, and $(-1, 1) \times (-1, 1) \times (-1, 1)$ in 1D, 2D, and 3D, respectively.

One can easily check that all four orthogonal projections in (2.3) and (2.4) commute with each other. We define the following new operators obtained from the products of these projections.

$$P_{e,x'}P_{e,y'}u(x', y') := \frac{1}{4}\{[u(x', y') + u(x', -y')] + [u(-x', y') + u(-x', -y')]\},$$

$$P_{e,x'}P_{o,y'}u(x', y') := \frac{1}{4}\{[u(x', y') - u(x', -y')] + [u(-x', y') - u(-x', -y')]\},$$

$$P_{o,x'}P_{o,y'}u(x', y') := \frac{1}{4}\{[u(x', y') - u(x', -y')] - [u(-x', y') - u(-x', -y')]\},$$

$$P_{o,x'}P_{e,y'}u(x', y') := \frac{1}{4}\{[u(x', y') + u(x', -y')] - [u(-x', y') + u(-x', -y')]\}.$$

Due to the aforementioned commutativity property, these are also orthogonal projections and satisfy the following decomposition property

$$P_{e,x'}P_{e,y'} + P_{e,x'}P_{o,y'} + P_{o,x'}P_{e,y'} + P_{o,x'}P_{o,y'} = I_{x',y'}. \tag{2.6}$$

These will be used in the definition of the novel operators in 2D.

Reflecting on the square support of the kernel function $\chi_\delta(x, y)$ in (2.1), we define the bulk of the domain as follows.

$$\text{bulk} = \{(x, y) \in \Omega : (x, y) \in (-1 + \delta, 1 - \delta) \times (-1 + \delta, 1 - \delta)\}.$$

We first prove that the operators $\mathcal{L}$ and $\mathcal{L}_{\text{orig}}$ agree in the bulk.

Lemma 2.1 *Suppose that u satisfies* (2.2). *Then,*

$$\mathcal{L}u(x, y) = \mathcal{L}_{orig}u(x, y), \quad (x, y) \in bulk.$$

Proof For $(x, y) \in$ bulk, we have

$$(x - \delta, x + \delta) \times (y - \delta, y + \delta) \cap \Omega = (x - \delta, x + \delta) \times (y - \delta, y + \delta).$$

Hence,

$$\iint_\Omega \widehat{C}(x'-x, y'-y)dx'dy' = \iint_\Omega \widehat{\chi_\delta}(x'-x, y'-y)\widehat{\mu}(x'-x, y'-y)dx'dy'$$

$$= \int_{x-\delta}^{x+\delta}\int_{y-\delta}^{y+\delta} \widehat{\mu}(x'-x, y'-y)dx'dy' = \int_{-\delta}^{\delta}\int_{-\delta}^{\delta} \mu(x', y')dx'dy'$$

$$= \iint_\Omega \chi_\delta(x', y')\mu(x', y')dx'dy' = \iint_\Omega C(x', y')dx'dy'.$$

The result follows. □

In the construction of the novel operators, a crucial ingredient is first restricting $\widehat{C}$ to Ω and then suitably extending it back to $\widehat{\Omega}$. To this end, we define the periodic,

antiperiodic, and mixed extensions of $C(x)$ from $(-1, 1)$ to $(-2, 2)$, respectively, as follows:

$$\widehat{C}_{\mathrm{p}}(x) := \begin{cases} C(x+2), & x \in (-2, -1), \\ C(x), & x \in (-1, 1), \\ C(x-2), & x \in (1, 2), \end{cases} \qquad \widehat{C}_{\mathrm{a}}(x) := \begin{cases} -C(x+2), & x \in (-2, -1), \\ C(x), & x \in (-1, 1), \\ -C(x-2), & x \in (1, 2). \end{cases}$$

We also utilize the following mixed extensions of $C(x)$.

$$\widehat{C}_{\mathrm{pa}}(x) := \begin{cases} C(x+2), & x \in (-2, -1), \\ C(x), & x \in (-1, 1), \\ -C(x-2), & x \in (1, 2), \end{cases} \qquad \widehat{C}_{\mathrm{ap}}(x) := \begin{cases} -C(x+2), & x \in (-2, -1), \\ C(x), & x \in (-1, 1), \\ C(x-2), & x \in (1, 2). \end{cases}$$

There is a slight abuse in the definition of the domain of the extensions. In fact, they are defined only on $(-2, 2) \setminus \{-1, 1\}$. However, these extensions enter into the formulation only as kernel functions of integral operators which allow their domains to differ by a set of measure zero.

Building on our 1D construction in [4], in higher dimensions, we discovered the operators that enforce local pure and mixed Neumann and Dirichlet BC. We can construct all possible 36 different types of BC and they are given in Section 6; see Tables 1, 2, 3 and 4. We present the main theorem in 2D with the following 4 types of BC.

Theorem 2.2 (*Main Theorem in 2D*) *Let* $\Omega := (-1, 1) \times (-1, 1)$ *and the kernel function be separable in the form*

$$C(x, y) = X(x)Y(y), \tag{2.7}$$

where X and Y are even functions. Then, the operators $\mathcal{M}_{\mathrm{N}}$, $\mathcal{M}_{\mathrm{D}}$, $\mathcal{M}_{\mathrm{N, DN}}$, and $\mathcal{M}_{\mathrm{ND, ND}}$ defined by

$$\left(\mathcal{M}_{\mathrm{N}} - c\right)u(x, y) := -\iint\limits_{\Omega} \left[\widehat{X}_{\mathrm{p}}(x'-x)P_{e,x'} + \widehat{X}_{\mathrm{a}}(x'-x)P_{o,x'}\right]$$
$$\left[\widehat{Y}_{\mathrm{p}}(y'-y)P_{e,y'} + \widehat{Y}_{\mathrm{a}}(y'-y)P_{o,y'}\right]u(x', y')dx'\,dy',$$

$$\left(\mathcal{M}_{\mathrm{D}} - c\right)u(x, y) := -\iint\limits_{\Omega} \left[\widehat{X}_{\mathrm{a}}(x'-x)P_{e,x'} + \widehat{X}_{\mathrm{p}}(x'-x)P_{o,x'}\right]$$
$$\left[\widehat{Y}_{\mathrm{a}}(y'-y)P_{e,y'} + \widehat{Y}_{\mathrm{p}}(y'-y)P_{o,y'}\right]u(x', y')dx'\,dy',$$

$$\left(\mathcal{M}_{\mathrm{N, DN}} - c\right)u(x, y) := -\iint\limits_{\Omega} \left[\widehat{X}_{\mathrm{p}}(x'-x)P_{e,x'} + \widehat{X}_{\mathrm{a}}(x'-x)P_{o,x'}\right]$$
$$\left[\widehat{Y}_{\mathrm{pa}}(y'-y)P_{e,y'} + \widehat{Y}_{\mathrm{ap}}(y'-y)P_{o,y'}\right]u(x', y')dx'\,dy',$$

$$\left(\mathcal{M}_{\mathrm{ND, ND}} - c\right)u(x, y) := -\iint\limits_{\Omega} \left[\widehat{X}_{\mathrm{ap}}(x'-x)P_{e,x'} + \widehat{X}_{\mathrm{pa}}(x'-x)P_{o,x'}\right]$$
$$\left[\widehat{Y}_{\mathrm{ap}}(y'-y)P_{e,y'} + \widehat{Y}_{\mathrm{pa}}(y'-y)P_{o,y'}\right]u(x', y')dx'\,dy'$$

agree with $\mathcal{L}u(x, y)$ *in the bulk, i.e., for* $(x, y) \in (-1 + \delta, 1 - \delta) \times (-1 + \delta, 1 - \delta)$. *Furthermore, the operators* $\mathcal{M}_N$ *and* $\mathcal{M}_D$ *enforce pure Neumann and Dirichlet BC, respectively:*

$$\frac{\partial}{\partial n}\big[(\mathcal{M}_N - c)u\big](x, \pm 1) = \frac{\partial}{\partial n}\big[(\mathcal{M}_N - c)u\big](\pm 1, y) = 0,$$

$$(\mathcal{M}_D - c)u(x, \pm 1) = (\mathcal{M}_D - c)u(\pm 1, y) = 0.$$

The operators $\mathcal{M}_{N, DN}$ *and* $\mathcal{M}_{ND, ND}$ *enforce mixed Neumann and Dirichlet BC, respectively, in the following way:*

$$\frac{\partial}{\partial n}\big[(\mathcal{M}_{N, DN} - c)u\big](\pm 1, y) = \frac{\partial}{\partial n}\big[(\mathcal{M}_{N, DN} - c)u\big](x, +1) = 0,$$
$$(\mathcal{M}_{N, DN} - c)u(x, -1) = 0,$$

and

$$\frac{\partial}{\partial n}\big[(\mathcal{M}_{ND, ND} - c)u\big](-1, y) = \frac{\partial}{\partial n}\big[(\mathcal{M}_{ND, ND} - c)u\big](x, -1) = 0,$$

$$(\mathcal{M}_{ND, ND} - c)u(+1, y) = (\mathcal{M}_{ND, ND} - c)u(x, +1) = 0.$$

Proof The proofs of agreement in the bulk and the verification of BC are given in Sections 4 and 5, respectively. For the BC configurations, see Section 6. $\qquad\square$

Remark 2.3 Although we assume a separable kernel function as in (2.7), note that we do not impose a separability assumption on the solution $u(x, y)$.

Remark 2.4 Although removing the assumption of separability does not seem to be possible at the analytic level, our ultimate goal is numerical approximation of problems involving our novel operators. That is why, in practice, discretized forms of the operators are more relevant to our purposes. Accommodating the separability assumption at the discrete level is the subject of ongoing work. To elaborate, let $C^h(x, y)$ denote the discretized form of a general kernel function $C(x, y)$. It is possible to find functions $X_i^h(x)$ and $Y_i^h(y)$ such that $C^h(x, y) \approx \sum_i X_i^h(x)Y_i^h(y)$ in some sense. This approximation is in the spirit of degenerate (a sum of separable) kernels in integral equations [20, 23]. One may then proceed with the kernel functions $X_i^h(x)Y_i^h(y)$ which satisfy the separability assumption.

Remark 2.5 The hallmark feature of a nonlocal solution is dispersion. With separable kernel functions, our solutions indeed exhibit dispersive behavior. See Fig. 10.

3 Operators in 1D

The operators $\mathcal{M}_N$ and $\mathcal{M}_D$ enforcing the pure Neumann and pure Dirichlet BC, respectively, have been reported in [4]. Here, we construct two additional operators $\mathcal{M}_{ND}$ and $\mathcal{M}_{DN}$ in 1D. We will extend all of these operators to higher dimensions in Sections 4 and 7. Thus, we find it instructive to provide the construction in 1D in full detail here.
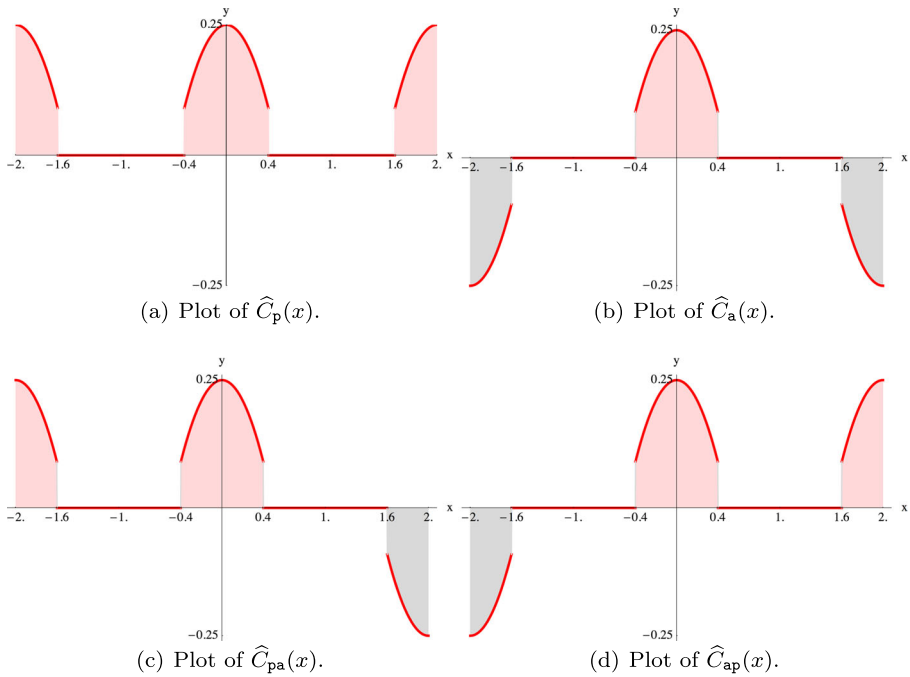
(a) Plot of $\widehat{C}_{\mathrm{p}}(x)$.

(b) Plot of $\widehat{C}_{\mathrm{a}}(x)$.

(c) Plot of $\widehat{C}_{\mathrm{pa}}(x)$.

(d) Plot of $\widehat{C}_{\mathrm{ap}}(x)$.

Fig. 1 The kernel function $C(x) = \chi_\delta(x)\mu(x)$ with $\delta = 0.4$ and $\mu(x) = 0.25 - x^2$. The periodic, antiperiodic, and mixed extensions of $C(x)$ are denoted by $\widehat{C}_{\mathrm{p}}(x)$, $\widehat{C}_{\mathrm{a}}(x)$, $\widehat{C}_{\mathrm{pa}}$, and $\widehat{C}_{\mathrm{ap}}$, respectively.

Following the construction in [1], we assume that $u, C \in L^2(\Omega)$ and define

$$\mathcal{C}_{\mathrm{p}}u(x) := \int_\Omega \widehat{C}_{\mathrm{p}}(x'-x)u(x')dx', \quad \mathcal{C}_{\mathrm{a}}u(x) := \int_\Omega \widehat{C}_{\mathrm{a}}(x'-x)u(x')dx', \quad (3.1)$$

$$\mathcal{C}_{\mathrm{pa}}u(x) := \int_\Omega \widehat{C}_{\mathrm{pa}}(x'-x)u(x')dx', \quad \mathcal{C}_{\mathrm{ap}}u(x) := \int_\Omega \widehat{C}_{\mathrm{ap}}(x'-x)u(x')dx'. \quad (3.2)$$

The only difference in the operators $\mathcal{C}_{\mathrm{p}}, \mathcal{C}_{\mathrm{a}}, \mathcal{C}_{\mathrm{pa}}$, and $\mathcal{C}_{\mathrm{ap}}$ is the extension type utilized for the kernel functions. We prove that the operators agree in the bulk by investigating how the corresponding kernel functions behave in the bulk. Also, see Figs. 1 and 2.

Lemma 3.1 *Let the kernel function $C(x)$ be in the form*

$$C(x) = \chi_\delta(x)\mu(x),$$

where $\mu(x) \in L^2(\Omega)$ is even. Let $\widehat{C}_{\mathrm{p}}(x)$, $\widehat{C}_{\mathrm{a}}(x)$, $\widehat{C}_{\mathrm{pa}}(x)$, and $\widehat{C}_{\mathrm{ap}}(x)$ denote the periodic, antiperiodic, and mixed extensions of $C(x)$ to $\widehat{\Omega} := (-2, 2)$, respectively. Then,

$$\widehat{C}_{\mathrm{p}}(x) = \widehat{C}_{\mathrm{a}}(x) = \widehat{C}_{\mathrm{pa}}(x) = \widehat{C}_{\mathrm{ap}}(x), \quad x \in (-2+\delta, 2-\delta).$$

Furthermore, we have the following agreement in the bulk. Namely, for $x \in (-1+\delta, 1-\delta)$,

$$\widehat{C}_{\mathrm{p}}(x'-x) = \widehat{C}_{\mathrm{a}}(x'-x) = \widehat{C}_{\mathrm{pa}}(x'-x) = \widehat{C}_{\mathrm{ap}}(x'-x), \quad x' \in (-1, 1). \quad (3.3)$$

(a) Plot of $\widehat{C}_{\mathrm{p}}(x, x')$.

(b) Plot of $\widehat{C}_{\mathrm{a}}(x, x')$.

(c) Plot of $\widehat{C}_{\mathrm{pa}}(x, x')$.

(d) Plot of $\widehat{C}_{\mathrm{ap}}(x, x')$.

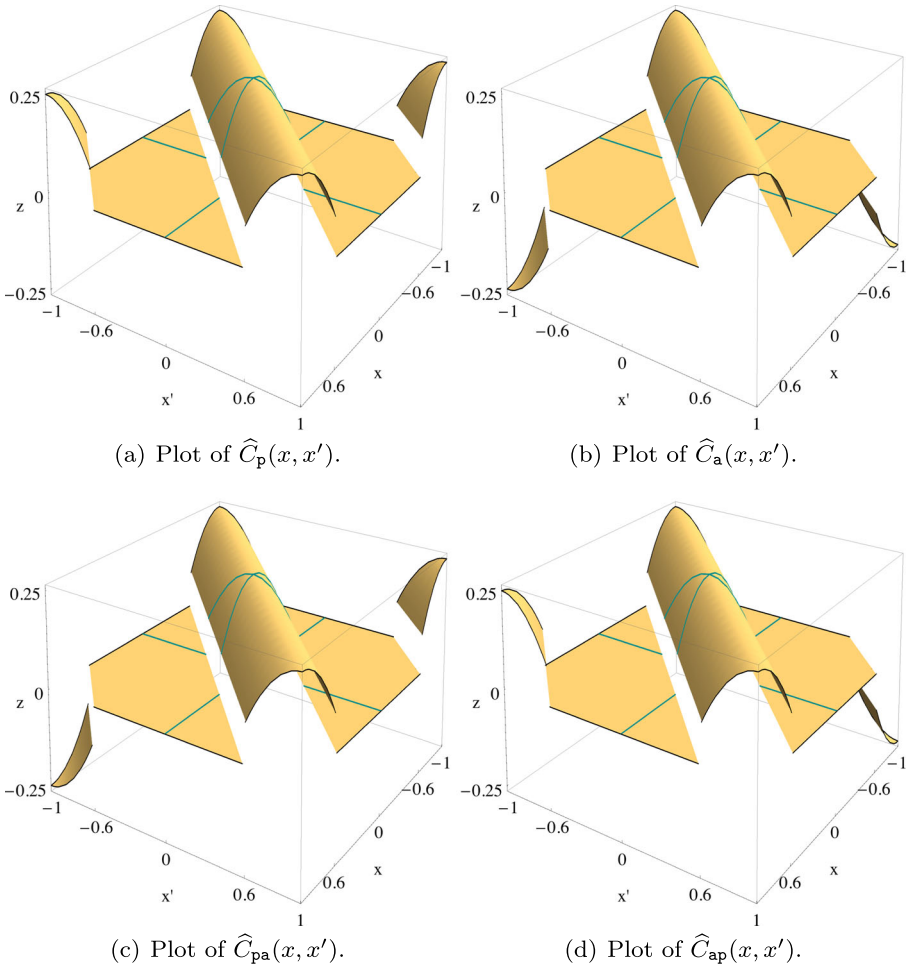**Fig. 2** For the same kernel function $C(x)$ in Fig. 1, we employ bivariate versions of $\widehat{C}_{\mathrm{p}}(x'-x)$, $\widehat{C}_{\mathrm{a}}(x'-x)$, $\widehat{C}_{\mathrm{pa}}(x'-x)$, and $\widehat{C}_{\mathrm{ap}}(x'-x)$ with the definition $\widehat{C}_{\mathrm{BC}}(x, x') := \widehat{C}_{\mathrm{BC}}(x'-x)$.

Proof See [4]. □

Using (3.3), we immediately obtain the following equivalence of operators in the bulk.

$$\mathcal{C}_{\mathrm{p}}u(x) = \mathcal{C}_{\mathrm{a}}u(x) = \mathcal{C}_{\mathrm{pa}}u(x) = \mathcal{C}_{\mathrm{ap}}u(x), \quad x \in (-1+\delta, 1-\delta). \qquad (3.4)$$

Even and odd parts of a univariate function $u(x)$ are used in the governing operators $\mathcal{M}_{\mathrm{N}}$, $\mathcal{M}_{\mathrm{D}}$, $\mathcal{M}_{\mathrm{ND}}$, and $\mathcal{M}_{\mathrm{DN}}$. We define the orthogonal projections that give the even and odd parts, respectively, of a univariate function by $P_e, P_o : L^2(\Omega) \to L^2(\Omega)$, whose definitions are

$$P_e u(x) := \frac{u(x) + u(-x)}{2}, \quad P_o u(x) := \frac{u(x) - u(-x)}{2}.$$

We present a commutativity property that allows us to identify the kernel functions associated to the operators $\mathcal{M}_N$ and $\mathcal{M}_D$.

Lemma 3.2

$$\mathcal{C}_p P_e = P_e \mathcal{C}_p, \quad \mathcal{C}_p P_o = P_o \mathcal{C}_p, \quad \mathcal{C}_a P_e = P_e \mathcal{C}_a, \quad \mathcal{C}_a P_o = P_o \mathcal{C}_a. \quad (3.5)$$

Proof We present the proof for $\mathcal{C}_p P_e = P_e \mathcal{C}_p$. The other results easily follow. We recall the definition of $\mathcal{C}_p u(x)$ in (3.1). We explicitly write $P_e \mathcal{C}_p u(x)$ and the result follows by utilizing the evenness of $\widehat{C}_p$ and a change of variable.

$$
\begin{aligned}
P_e \mathcal{C}_p u(x) &= \frac{1}{2} \left(\int_\Omega \widehat{C}_p(x'-x) u(x') dx' + \int_\Omega \widehat{C}_p(x'+x) u(x') dx' \right) \\
&= \frac{1}{2} \left(\int_\Omega \widehat{C}_p(x'-x) u(x') dx' + \int_\Omega \widehat{C}_p(x'-x) u(-x') dx' \right) \\
&= \int_\Omega \widehat{C}_p(x'-x) P_e u(x') dx' \\
&= \mathcal{C}_p P_e u(x). \qquad \square
\end{aligned}
$$

Remark 3.3 The commutativity property helps in identifying the associated kernel functions; see (3.7) and (3.8). Note that the above commutativity property does not hold for the operators $\mathcal{C}_{pa}$ and $\mathcal{C}_{ap}$. Identification of the associated kernel functions can be done by direct manipulation.

Theorem 3.4 *(**Main Theorem in 1D**) Let $c = \int_\Omega C(x') dx'$. The following operators $\mathcal{M}_N$, $\mathcal{M}_D$, $\mathcal{M}_{ND}$, and $\mathcal{M}_{DN}$ defined by*

$$(\mathcal{M}_N - c)u(x) := -\int_\Omega \left[\widehat{C}_p(x'-x) P_e u(x') + \widehat{C}_a(x'-x) P_o u(x') \right] dx',$$

$$(\mathcal{M}_D - c)u(x) := -\int_\Omega \left[\widehat{C}_a(x'-x) P_e u(x') + \widehat{C}_p(x'-x) P_o u(x') \right] dx',$$

$$(\mathcal{M}_{ND} - c)u(x) := -\int_\Omega \left[\widehat{C}_{ap}(x'-x) P_e u(x') + \widehat{C}_{pa}(x'-x) P_o u(x') \right] dx',$$

$$(\mathcal{M}_{DN} - c)u(x) := -\int_\Omega \left[\widehat{C}_{pa}(x'-x) P_e u(x') + \widehat{C}_{ap}(x'-x) P_o u(x') \right] dx'$$

agree with $\mathcal{L}u(x)$ in the bulk, i.e., for $x \in (-1+\delta, 1-\delta)$. Furthermore, the operators $\mathcal{M}_N$ and $\mathcal{M}_D$ enforce pure Neumann and Dirichlet BC, respectively:

$$\frac{d}{dx}\left[(\mathcal{M}_N - c)u \right](\pm 1) = 0,$$

$$(\mathcal{M}_D - c)u(\pm 1) = 0.$$

The operator $\mathcal{M}_{\text{ND}}$ and $\mathcal{M}_{\text{DN}}$ enforce mixed Neumann and Dirichlet BC, respectively:

$$\left(\mathcal{M}_{\text{ND}} - c\right)u(+1) = \frac{d}{dx}\left[\left(\mathcal{M}_{\text{ND}} - c\right)u\right](-1) = 0,$$

$$\left(\mathcal{M}_{\text{DN}} - c\right)u(-1) = \frac{d}{dx}\left[\left(\mathcal{M}_{\text{DN}} - c\right)u\right](+1) = 0.$$

We define the operators $\mathcal{M}_{\text{N}}$, $\mathcal{M}_{\text{D}}$, $\mathcal{M}_{\text{ND}}$, and $\mathcal{M}_{\text{DN}}$ as densely defined, linear, bounded, and self-adjoint operators. More precisely, $\mathcal{M}_{\text{D}}, \mathcal{M}_{\text{N}}, \mathcal{M}_{\text{ND}}, \mathcal{M}_{\text{DN}} \in L\left(L^2(\Omega), L^2(\Omega)\right)$. Imposing Neumann (also periodic and antiperiodic) BC requires differentiation. For technical details regarding differentiation under the integral sign, see the discussion on the Leibniz Rule in [4] whose proof relies on the Lebesgue Dominated Convergence Theorem. In addition, the limit in the definition of the Dirichlet BC can be interchanged with the integral sign, again by the Lebesgue Dominated Convergence Theorem.

Remark 3.5 When we assume homogeneous Neumann and Dirichlet BC on u, then the operators $\mathcal{M}_{\text{N}}$ and $\mathcal{M}_{\text{D}}$ enforce homogeneous Neumann and Dirichlet BC, respectively. More precisely, for $u'(\pm 1) = 0$ and $u(\pm 1) = 0$, we obtain $\frac{d}{dx}\mathcal{M}_{\text{N}}u(\pm 1) = 0$ and $\mathcal{M}_{\text{D}}u(\pm 1) = 0$, respectively. The same line of argument applies to the operators $\mathcal{M}_{\text{ND}}$ and $\mathcal{M}_{\text{DN}}$.

Using the operators $\mathcal{C}_{\text{p}}$, $\mathcal{C}_{\text{a}}$, $\mathcal{C}_{\text{pa}}$, and $\mathcal{C}_{\text{ap}}$ given in (3.1) and (3.2), we can express the operators $\mathcal{M}_{\text{N}}$, $\mathcal{M}_{\text{D}}$, $\mathcal{M}_{\text{ND}}$, and $\mathcal{M}_{\text{DN}}$ in the following way.

$$\mathcal{M}_{\text{N}} - c = -\left(\mathcal{C}_{\text{p}} P_e + \mathcal{C}_{\text{a}} P_o\right), \qquad \mathcal{M}_{\text{D}} - c = -\left(\mathcal{C}_{\text{a}} P_e + \mathcal{C}_{\text{p}} P_o\right),$$

$$\mathcal{M}_{\text{ND}} - c = -\left(\mathcal{C}_{\text{ap}} P_e + \mathcal{C}_{\text{pa}} P_o\right), \quad \mathcal{M}_{\text{DN}} - c = -\left(\mathcal{C}_{\text{pa}} P_e + \mathcal{C}_{\text{ap}} P_o\right).$$

Using the commutativity property (3.5), we arrive at the following representation.

$$\mathcal{M}_{\text{N}} - c = -\left(P_e \mathcal{C}_{\text{p}} + P_o \mathcal{C}_{\text{a}}\right), \quad \mathcal{M}_{\text{D}} - c = -\left(P_e \mathcal{C}_{\text{a}} + P_o \mathcal{C}_{\text{p}}\right).$$

Now, we can identify the kernel functions associated to operators $\mathcal{M}_{\text{N}}$ and $\mathcal{M}_{\text{D}}$.

$$\left(\mathcal{M}_{\text{N}} - c\right)u(x) = -\int_{\Omega} K_{\text{N}}(x, x')u(x')dx',$$

$$\left(\mathcal{M}_{\text{D}} - c\right)u(x) = -\int_{\Omega} K_{\text{D}}(x, x')u(x')dx', \tag{3.6}$$

where

$$K_{\text{N}}(x, x') := \frac{1}{2}\left\{\left[\widehat{C}_{\text{p}}(x'-x) + \widehat{C}_{\text{p}}(x'+x)\right] + \left[\widehat{C}_{\text{a}}(x'-x) - \widehat{C}_{\text{a}}(x'+x)\right]\right\}, \tag{3.7}$$

$$K_{\text{D}}(x, x') := \frac{1}{2}\left\{\left[\widehat{C}_{\text{a}}(x'-x) + \widehat{C}_{\text{a}}(x'+x)\right] + \left[\widehat{C}_{\text{p}}(x'-x) - \widehat{C}_{\text{p}}(x'+x)\right]\right\}. \tag{3.8}$$

We also want to identify the integrands associated to the operators $\mathcal{M}_{\mathrm{ND}}$ and $\mathcal{M}_{\mathrm{DN}}$. We proceed by direct manipulation. By writing P_e and P_o explicitly and utilizing a simple change of variable, we arrive at the following expressions.

$$(\mathcal{M}_{\mathrm{ND}} - c)u(x) = -\int_{\Omega} K_{\mathrm{ND}}(x, x')u(x')dx',$$

$$(\mathcal{M}_{\mathrm{DN}} - c)u(x) = -\int_{\Omega} K_{\mathrm{DN}}(x, x')u(x')dx',$$

where

$$K_{\mathrm{ND}}(x, x') := \frac{1}{2}\{[\widehat{C}_{\mathrm{pa}}(x'-x) + \widehat{C}_{\mathrm{pa}}(x'+x)] + [\widehat{C}_{\mathrm{ap}}(x'-x) - \widehat{C}_{\mathrm{ap}}(x'+x)]\},$$

$$K_{\mathrm{DN}}(x, x') := \frac{1}{2}\{[\widehat{C}_{\mathrm{ap}}(x'-x) + \widehat{C}_{\mathrm{ap}}(x'+x)] + [\widehat{C}_{\mathrm{pa}}(x'-x) - \widehat{C}_{\mathrm{pa}}(x'+x)]\}.$$

In order to align with the construction given in [1], we assume that $C(x) \in L^2(\Omega)$, and hence,

$$\widehat{C}_{\mathrm{a}}(x), \ \widehat{C}_{\mathrm{p}}(x), \ \widehat{C}_{\mathrm{pa}}(x), \ \text{and} \widehat{C}_{\mathrm{ap}}(x) \in L^2(\widehat{\Omega}). \tag{3.9}$$

Remark 3.6 The boundedness of $\mathcal{M}_{\mathrm{N}}, \mathcal{M}_{\mathrm{D}}, \mathcal{M}_{\mathrm{ND}}$, and $\mathcal{M}_{\mathrm{DN}}$ follow from the choices of (2.2) and (3.9). In addition, all of them fall into the class of integral operators; hence, their self-adjointness follows from the fact that the corresponding kernels are symmetric (due to evenness of C), i.e., $K_{\mathrm{BC}}(x, x') = K_{\mathrm{BC}}(x', x)$ and $\mathrm{BC} \in \{\mathrm{N}, \mathrm{D}, \mathrm{ND}, \mathrm{DN}\}$. The cases of $\mathrm{BC} \in \{\mathrm{ND}, \mathrm{DN}\}$ are more involved than the rest. One useful identity is $\widehat{C}_{\mathrm{ap}}(x'-x) = \widehat{C}_{\mathrm{pa}}(-x'+x)$.

3.1 Operator-theoretic treatment of the governing equation

In this subsection, we present the operator theoretic treatment of the following governing equation. For the sake of clarity, we restrict the discussion to the case of Dirichlet BC:

$$\mathcal{M}_{\mathrm{D}}u(x) = b(x), \quad x \in \Omega, \tag{3.10a}$$

$$u(\pm 1) = 0. \tag{3.10b}$$

Here, $b(x)$ is a forcing function that satisfies the compatibility condition [4, Sec. 5]

$$\lim_{x \to \pm 1} b(x) = c \lim_{x \to \pm 1} u(x).$$

Since (3.10) is a boundary value problem, it naturally assumes the existence of $\lim_{x \to \pm 1} u(x)$. Although $\mathcal{M}_{\mathrm{D}}$ acts on $u \in L^2(\Omega)$, which ignores the values of u on the boundary of Ω, it is designed in a way that the solution of (3.10a) respects the BC (3.10b). We explain this in the remainder of this subsection.

The governing operator $\mathcal{M}_{\mathrm{D}}$ is linear and self-adjoint. In addition, it possesses two more properties relevant to satisfying the BC: it is *densely defined and bounded*. A densely defined operator exploits density of spaces and the dense space should take the BC into account. It is well-known that $C^m(\overline{\Omega})$ is dense in $L^2(\Omega)$ for any $m \in \mathbb{N}$. For the case of Dirichlet BC, the appropriate choice turns out to be $m = 2$.

Let us briefly explain how we employ the operator theory to treat a densely defined and bounded operator for the boundary value problem (3.10). We begin with restricting the governing operator to the dense space of choice $C^2(\overline{\Omega})$. We seek the solution to (3.10) with $u \in C^2(\overline{\Omega})$ with the restricted governing operator $\mathcal{M}_D|_{C^2(\overline{\Omega})}$ which is essentially self-adjoint, i.e., its closure is self-adjoint. The operator $\mathcal{M}_D|_{C^2(\overline{\Omega})}$ is bounded and $C^2(\overline{\Omega})$ is dense in $L^2(\Omega)$. Hence, the operator $\mathcal{M}_D|_{C^2(\overline{\Omega})}$ has a unique bounded extension to $L^2(\Omega)$. This explains how the operator is extended from $C^2(\overline{\Omega})$ to $L^2(\Omega)$ using the density argument.

Finally, to make sure that the limits of the left hand side of (3.10a) exist, we write it as

$$\lim_{x \to \pm 1} (\mathcal{M}_D - c)u(x) + c \lim_{x \to \pm 1} u(x) = \lim_{x \to \pm 1} b(x).$$

One crucial question remains: Why do the limits

$$\lim_{x \to \pm 1} (\mathcal{M}_D - c)u(x) \tag{3.11}$$

exist? The answer is due to a subtle point in our construction. The bounded operator $\mathcal{M}_D$ after subtracting c, i.e., $\mathcal{M}_D - c$, possesses the Hilbert-Schmidt property. As a result, given $u \in L^2(\Omega)$, the function $(\mathcal{M}_D - c)u$ has an extension to a continuous function on $\overline{\Omega}$. Consequently, the limits in (3.11) exist and in fact are equal to 0. To see the latter, we expand u in the Hilbert basis as $u(x) = \sum_{k=1}^{\infty} \langle e_k^D | u \rangle e_k^D(x)$. By the spectral theorem for bounded operators, we have

$$\lim_{x \to \pm 1} (\mathcal{M}_D - c)u(x) = \lim_{x \to \pm 1} \sum_{k=1}^{\infty} (\lambda_k(\mathcal{M}_D) - c)\langle e_k^D | u \rangle e_k^D(x)$$

$$= \sum_{k=1}^{\infty} (\lambda_k(\mathcal{M}_D) - c)\langle e_k^D | u \rangle \underbrace{\lim_{x \to \pm 1} e_k^D(x)}_{=0}$$

$$= 0$$

The interchange of $\lim_{x \to \pm 1}$ with $\sum_{k=1}^{\infty}$ is justified by the uniform convergence due to the Hilbert-Schmidt property. For details, see [2, 6, 7].

3.2 Proof of Theorem 3.4

In the upcoming proofs, we want to report a minor caveat. We use $\widehat{C}_a(x' + 1) = -\widehat{C}_a(x' - 1)$ which holds for $x' \neq 0$. For $x' = 0$, i.e., $\widehat{C}_a(x' + 1) = C(1) \neq -C(-1) = -\widehat{C}_a(x' - 1)$. Since $x' = 0$ is only a point, it does not change the value of the integration. We choose not to point it out each time we run into this case.

Proof The key observation that leads to the agreement of the operators $\mathcal{M}_N$, $\mathcal{M}_D$, $\mathcal{M}_{ND}$, and $\mathcal{M}_{DN}$ with the operator $\mathcal{L}$ is the agreement of kernel functions in (3.3). To account for the convolution present in the the governing operators, we define a generic operator

$$\mathcal{C}u(x) := \int_{\Omega} \widehat{C}(x' - x)u(x')dx'.$$

The property (3.3) leads to the equivalence (3.4). Hence, the other operators agree in the bulk. For $x \in (-1 + \delta, 1 - \delta)$, we have

$$\begin{aligned}
\mathcal{L} - c &= -\mathcal{C} \\
&= -\mathcal{C}(P_e + P_o) && \text{since } I = P_e + P_o \\
&= -(\mathcal{C}P_e + \mathcal{C}P_o) \\
&= -(\mathcal{C}_{\mathrm{p}}P_e + \mathcal{C}_{\mathrm{a}}P_o) &&=: \mathcal{M}_{\mathrm{N}} - c \quad \text{by (3.4)} && (3.12) \\
&= -(\mathcal{C}_{\mathrm{a}}P_e + \mathcal{C}_{\mathrm{p}}P_o) &&=: \mathcal{M}_{\mathrm{D}} - c && (3.13) \\
&= -(\mathcal{C}_{\mathrm{ap}}P_e + \mathcal{C}_{\mathrm{pa}}P_o) &&=: \mathcal{M}_{\mathrm{ND}} - c && (3.14) \\
&= -(\mathcal{C}_{\mathrm{pa}}P_e + \mathcal{C}_{\mathrm{ap}}P_o) &&=: \mathcal{M}_{\mathrm{DN}} - c. && (3.15)
\end{aligned}$$

Here, the first three identities hold regardless of the extension type, that is why the subscript is suppressed.

First, we prove that the operators $\mathcal{M}_{\mathrm{N}}$ and $\mathcal{M}_{\mathrm{D}}$ enforce pure Neumann and Dirichlet BC, respectively. Next, we will prove that the operators $\mathcal{M}_{\mathrm{ND}}$ and $\mathcal{M}_{\mathrm{DN}}$ enforce mixed Neumann and Dirichlet BC, respectively.

- **The operator $\mathcal{M}_{\mathrm{N}}$** First we remove the points at which the derivative of $K_{\mathrm{N}}(x, x')$ does not exist from the set of integration. Note that such points form a set of measure zero, and hence, does not affect the value of the integral. We differentiate both sides of (3.6). In [4], we had proved that the differentiation in the definition of the Neumann BC can interchange with the integral. We can differentiate the integrand $K_{\mathrm{N}}(x, x')$ piecewise and obtain

$$\frac{d}{dx}\big[(\mathcal{M}_{\mathrm{N}} - c)u\big](x) = -\int_{\Omega} \frac{\partial K_{\mathrm{N}}}{\partial x}(x, x')u(x')dx', \qquad (3.16)$$

where

$$\frac{\partial K_{\mathrm{N}}}{\partial x}(x, x') = \frac{1}{2}\big\{\big[-\widehat{C}'_{\mathrm{p}}(x'-x) + \widehat{C}'_{\mathrm{p}}(x'+x)\big] + \big[-\widehat{C}'_{\mathrm{a}}(x'-x) - \widehat{C}'_{\mathrm{a}}(x'+x)\big]\big\}.$$

We check the boundary values by plugging $x = \pm 1$ in (3.16).

$$\frac{d}{dx}\big[(\mathcal{M}_{\mathrm{N}} - c)u\big](\pm 1) = -\int_{\Omega} \frac{\partial K_{\mathrm{N}}}{\partial x}(\pm 1, x')u(x')dx'. \qquad (3.17)$$

The functions $\widehat{C}'_{\mathrm{p}}$ and $\widehat{C}'_{\mathrm{a}}$ are 2-periodic and 2-antiperiodic because they are the derivatives of 2-periodic and 2-antiperiodic functions, respectively. Hence,

$$\widehat{C}'_{\mathrm{p}}(x' \mp 1) = \widehat{C}'_{\mathrm{p}}(x' \pm 1) \quad \text{and} \quad \widehat{C}'_{\mathrm{a}}(x' \mp 1) = -\widehat{C}'_{\mathrm{a}}(x' \pm 1).$$

Hence, the integrand in (3.17) vanishes, i.e.,

$$\frac{\partial K_{\mathrm{N}}}{\partial x}(\pm 1, x') = 0.$$

Therefore, we arrive at

$$\frac{d}{dx}\mathcal{M}_{\mathrm{N}}u(\pm 1) = cu'(\pm 1).$$

When we assume that u satisfies homogeneous Neumann BC, i.e., $u'(\pm 1) = 0$, we conclude that the operator $\mathcal{M}_{\mathrm{N}}$ enforces homogeneous Neumann BC as well.

- **The operator $\mathcal{M}_D$** By the Lebesgue Dominated Convergence Theorem, the limit in the definition of the Dirichlet BC can be interchanged with the integral. Now, we check the boundary values by plugging $x = \pm 1$ in (3.8).

$$\left(\mathcal{M}_D - c\right)u(\pm 1) = -\int_\Omega K_D(\pm 1, x')u(x')dx'. \qquad (3.18)$$

Since $\widehat{C}_p$ and $\widehat{C}_a$ are 2-periodic and 2-antiperiodic, respectively, we have

$$\widehat{C}_p(x' \mp 1) = \widehat{C}_p(x' \pm 1) \quad \text{and} \quad \widehat{C}_a(x' \mp 1) = -\widehat{C}_a(x' \pm 1).$$

Hence, the integrand in (3.18) vanishes, i.e., $K_D(\pm 1, x') = 0$. Therefore, we arrive at

$$\mathcal{M}_D u(\pm 1) = cu(\pm 1).$$

When we assume that u satisfies homogeneous Dirichlet BC, i.e., $u(\pm 1) = 0$, we conclude that the operator $\mathcal{M}_D$ enforces homogeneous Dirichlet BC as well.

- **The operator $\mathcal{M}_{ND}$** First we prove that $\mathcal{C}_{ap}P_eu(+1) = 0$. We use a change of variable in the second piece.

$$\mathcal{C}_{ap}P_eu(+1) = \frac{1}{2}\left(\int_\Omega \widehat{C}_{ap}(x'-1)P_eu(x')dx' + \int_\Omega \widehat{C}_{ap}(-x'-1)P_eu(x')dx'\right).$$

Then, we split the integrals into two parts as follows.

$$\mathcal{C}_{ap}P_eu(+1) = \frac{1}{2}\int_{-1}^0 \left[\widehat{C}_{ap}(x'-1) + \widehat{C}_{ap}(-x'-1)\right]P_eu(x')dx'$$
$$+ \frac{1}{2}\int_0^1 \left[\widehat{C}_{ap}(x'-1) + \widehat{C}_{ap}(-x'-1)\right]P_eu(x')dx'. \quad (3.19)$$

For $x' \in (-1, 0)$, we have $x' - 1 \in (-2, -1)$. By using the definition of $\widehat{C}_{ap}$ and the evenness of C, we obtain

$$\widehat{C}_{ap}(x'-1) = -\widehat{C}_{ap}(x'+1) = -C(x'+1) = -C(-x'-1) = -\widehat{C}_{ap}(-x'-1).$$
$$(3.20)$$

For $x' \in (0, 1)$, we have $x' - 1 \in (-1, 0)$. By using the definition of $\widehat{C}_{ap}$ and the evenness of C, we obtain

$$\widehat{C}_{ap}(x'-1) = C(x'-1) = C(-x'+1) = -\widehat{C}_{ap}(-x'-1). \qquad (3.21)$$

Combining (3.20) and (3.21) with (3.19), we conclude that $\mathcal{C}_{ap}P_eu(+1) = 0$. Similarly, we can conclude that $\mathcal{C}_{pa}P_ou(+1) = 0$. Consequently, we arrive at

$$\mathcal{C}_{ND}u(+1) = 0.$$

We prove that $\dfrac{d}{dx}\mathcal{C}_{pa}P_ou(-1) = 0$. We use a change of variable in the second piece.

$$\frac{d}{dx}\mathcal{C}_{pa}P_ou(-1) = -\frac{1}{2}\left(\int_\Omega \widehat{C}'_{pa}(x'+1)P_ou(x')dx' - \int_\Omega \widehat{C}'_{pa}(-x'+1)P_ou(x')dx'\right).$$

Then, we split the integrals into two parts as follows.

$$\frac{d}{dx}\mathcal{C}_{\mathrm{pa}}P_o u(-1) = -\frac{1}{2}\int_{-1}^{0}\left[\widehat{C}'_{\mathrm{pa}}(x'+1) - \widehat{C}'_{\mathrm{pa}}(-x'+1)\right]P_o u(x')dx'$$
$$-\frac{1}{2}\int_{0}^{1}\left[\widehat{C}'_{\mathrm{pa}}(x'+1) - \widehat{C}'_{\mathrm{pa}}(-x'+1)\right]P_o u(x')dx'. \tag{3.22}$$

For $x' \in (-1, 0)$, we have $x' + 1 \in (0, 1)$. By using the definition of $\widehat{C}_{\mathrm{pa}}$ and the oddness of C', we obtain

$$\widehat{C}'_{\mathrm{pa}}(x'+1) = C'(x'+1) = -C'(-x'-1) = -\widehat{C}'_{\mathrm{pa}}(-x'-1) = \widehat{C}'_{\mathrm{pa}}(-x'+1). \tag{3.23}$$

For $x' \in [0, 1]$, we have $x' + 1 \in (1, 2)$. By using the definition of $\widehat{C}_{\mathrm{pa}}$ and the oddness of C', we obtain

$$\widehat{C}'_{\mathrm{pa}}(x'+1) = -\widehat{C}'_{\mathrm{pa}}(x'-1) = -C'(x'-1) = C'(-x'+1) = \widehat{C}'_{\mathrm{pa}}(-x'+1). \tag{3.24}$$

Combining (3.23) and (3.24) with (3.22), we conclude that $\frac{d}{dx}\mathcal{C}_{\mathrm{pa}}P_o u(-1) = 0$. Similarly, we can conclude that $\frac{d}{dx}\mathcal{C}_{\mathrm{ap}}P_e u(-1) = 0$. Consequently, we arrive at

$$\frac{d}{dx}\mathcal{C}_{\mathrm{ND}}u(-1) = 0.$$

- **The operator $\mathcal{M}_{\mathrm{DN}}$:** The proof is similar to the case of $\mathcal{M}_{\mathrm{ND}}$. □

Remark 3.7 As we prepare to construct the operators in 2D, it is useful to explicitly denote the variable x' on which P_e and P_o act in the following way.

$$\mathcal{C}_{\mathrm{N}}u(x) := \left(\mathcal{C}_{\mathrm{p}}P_{e,x'} + \mathcal{C}_{\mathrm{a}}P_{o,x'}\right)u(x)$$
$$\mathcal{C}_{\mathrm{D}}u(x) := \left(\mathcal{C}_{\mathrm{a}}P_{e,x'} + \mathcal{C}_{\mathrm{p}}P_{o,x'}\right)u(x)$$
$$\mathcal{C}_{\mathrm{ND}}u(x) := \left(\mathcal{C}_{\mathrm{ap}}P_{e,x'} + \mathcal{C}_{\mathrm{pa}}P_{o,x'}\right)u(x)$$
$$\mathcal{C}_{\mathrm{DN}}u(x) := \left(\mathcal{C}_{\mathrm{pa}}P_{e,x'} + \mathcal{C}_{\mathrm{ap}}P_{o,x'}\right)u(x).$$

Consequently, checking if the operators enforce the BC reduces to obtaining

$$\begin{aligned}
\frac{d}{dx}\mathcal{C}_{\mathrm{N}}u(\pm 1) &= 0, & \mathcal{C}_{\mathrm{D}}u(\pm 1) &= 0 \\
\frac{d}{dx}\mathcal{C}_{\mathrm{ND}}u(-1) &= 0, & \mathcal{C}_{\mathrm{ND}}u(+1) &= 0 \\
\frac{d}{dx}\mathcal{C}_{\mathrm{DN}}u(+1) &= 0, & \mathcal{C}_{\mathrm{DN}}u(-1) &= 0.
\end{aligned} \tag{3.25}$$

4 The construction of 2D operators

We begin with defining the following auxiliary operators that act on a bivariate function

$$\mathcal{X}_{\mathrm{E}}u(x, y) = \int_{\Omega} \widehat{X}_{\mathrm{E}}(x'-x)u(x', y)dx', \quad \mathcal{Y}_{\mathrm{E}}u(x, y) = \int_{\Omega} \widehat{Y}_{\mathrm{E}}(y'-y)u(x, y')dy',$$

where the extension type $\mathrm{E} \in \{\mathrm{p}, \mathrm{a}, \mathrm{pa}, \mathrm{ap}\}$. When a particular identity holds independently of the extension type, the subscript is suppressed. Using the separability assumption (2.7) on the kernel function, we have

$$\widehat{C}(x, y) = \widehat{X}(x)\widehat{Y}(y). \tag{4.1}$$

To account for the convolution present in the the governing operators, we define a generic operator

$$\mathcal{C}u(x, y) = \iint_{\Omega} \widehat{C}(x'-x, y'-y)u(x', y')dx'dy'. \tag{4.2}$$

The separability of the kernel function (4.1) and the Fubini Theorem lead to an important commutativity property:

$$\begin{aligned}
\mathcal{C}u(x, y) &= \iint_{\Omega} \widehat{X}(x'-x)\widehat{Y}(y'-y)u(x', y')dx'dy' \\
&= \int_{\Omega} \widehat{X}(x'-x)\Big(\int_{\Omega} \widehat{Y}(y'-y)u(x', y')dy'\Big)dx' \\
&= \int_{\Omega} \widehat{X}(x'-x)\Big(\mathcal{Y}u(x', y)\Big)dx' \\
&= \mathcal{X}\big(\mathcal{Y}u\big)(x, y). \tag{4.3}
\end{aligned}$$

On the other hand, a change in the order of integration leads to

$$\mathcal{C}u(x, y) = \mathcal{Y}\big(\mathcal{X}u\big)(x, y). \tag{4.4}$$

As a by-product, we also see that $\mathcal{C}$ can be decomposed into a product of two 1D operators where the action of $\mathcal{X}$ and $\mathcal{Y}$ are on the variables x and y, respectively. These two properties are instrumental in satisfying the BC as will be detailed in Section 5.

Similar to (3.4), we also obtain the following equivalence of operators in the bulk. For fixed y_0 and $x \in (-1 + \delta, 1 - \delta)$, we have

$$\mathcal{X}_{\mathrm{p}}u(x, y_0) = \mathcal{X}_{\mathrm{a}}u(x, y_0) = \mathcal{X}_{\mathrm{pa}}u(x, y_0) = \mathcal{X}_{\mathrm{ap}}u(x, y_0).$$

Also, for fixed x_0 and $y \in (-1 + \delta, 1 - \delta)$, we have

$$\mathcal{Y}_{\mathrm{p}}u(x_0, y) = \mathcal{Y}_{\mathrm{a}}u(x_0, y) = \mathcal{Y}_{\mathrm{pa}}u(x_0, y) = \mathcal{Y}_{\mathrm{ap}}u(x_0, y).$$

The choice made in (3.12) leads to the construction of the operator that enforces pure Neumann BC in the x- and y-variable as follows.

$$\mathcal{X}_N := \mathcal{X}_p P_{e,x'} + \mathcal{X}_a P_{o,x'} \quad \text{(in the } x\text{-variable)} \tag{4.5}$$

$$\mathcal{Y}_N := \mathcal{Y}_p P_{e,y'} + \mathcal{Y}_a P_{o,y'} \quad \text{(in the } y\text{-variable).} \tag{4.6}$$

Similarly, the choice made in (3.13) leads to the construction of the operator that enforces pure Dirichlet BC in the x- and y-variable as follows.

$$\mathcal{X}_D := \mathcal{X}_a P_{e,x'} + \mathcal{X}_p P_{o,x'} \quad \text{(in the } x\text{-variable)} \tag{4.7}$$

$$\mathcal{Y}_D := \mathcal{Y}_a P_{e,y'} + \mathcal{Y}_p P_{o,y'} \quad \text{(in the } y\text{-variable).} \tag{4.8}$$

Similarly, the choices made in (3.14) and (3.15) lead to the construction of the operators that enforce mixed Neumann-Dirichlet and Dirichlet-Neumann BC in the x- and y-variable as follows.

$$\mathcal{X}_{ND} := \mathcal{X}_{ap} P_{e,x'} + \mathcal{X}_{pa} P_{o,x'} \quad \text{(in the } x\text{-variable)} \tag{4.9}$$

$$\mathcal{Y}_{ND} := \mathcal{Y}_{ap} P_{e,y'} + \mathcal{Y}_{pa} P_{o,y'} \quad \text{(in the } y\text{-variable)} \tag{4.10}$$

$$\mathcal{X}_{DN} := \mathcal{X}_{pa} P_{e,x'} + \mathcal{X}_{ap} P_{o,x'} \quad \text{(in the } x\text{-variable)} \tag{4.11}$$

$$\mathcal{Y}_{DN} := \mathcal{Y}_{pa} P_{e,y'} + \mathcal{Y}_{ap} P_{o,y'} \quad \text{(in the } y\text{-variable).} \tag{4.12}$$

We want to construct an operator that enforces pure Neumann BC on the square. We make the choice that gives the 1D Neumann operator both in x- and y-variables. Hence, combining (4.5) and (4.6), we define the 2D pure Neumann operator as

$$\mathcal{M}_N - c := -\mathcal{X}_N \mathcal{Y}_N = -\big(\mathcal{X}_p P_{e,x'} + \mathcal{X}_a P_{o,x'}\big)\big(\mathcal{Y}_p P_{e,y'} + \mathcal{Y}_a P_{o,y'}\big). \tag{4.13}$$

Similarly, combining (4.7) and (4.8), we define the 2D pure Dirichlet operator as

$$\mathcal{M}_D - c := -\mathcal{X}_D \mathcal{Y}_D = -\big(\mathcal{X}_a P_{e,x'} + \mathcal{X}_p P_{o,x'}\big)\big(\mathcal{Y}_a P_{e,y'} + \mathcal{Y}_p P_{o,y'}\big). \tag{4.14}$$

Similarly, combining (4.9), (4.10), (4.11), and (4.12), we define the 2D mixed operators as follows.

$$\mathcal{M}_{N,DN} - c := -\mathcal{X}_N \mathcal{Y}_{DN} = -\big(\mathcal{X}_p P_{e,x'} + \mathcal{X}_a P_{o,x'}\big)\big(\mathcal{Y}_{pa} P_{e,y'} + \mathcal{Y}_{ap} P_{o,y'}\big) \tag{4.15}$$

$$\mathcal{M}_{ND,ND} - c := -\mathcal{X}_{ND} \mathcal{Y}_{ND} = -\big(\mathcal{X}_{ap} P_{e,x'} + \mathcal{X}_{pa} P_{o,x'}\big)\big(\mathcal{Y}_{ap} P_{e,y'} + \mathcal{Y}_{pa} P_{o,y'}\big). \tag{4.16}$$

All possible 36 types of BC are given in Section 6.

Recalling (1.1), we immediately see that the operator $\mathcal{L}$ agrees in the bulk with the operators given above. Namely,

$$\mathcal{L} - c = -\mathcal{C} = \mathcal{M}_N - c = \mathcal{M}_D - c = \mathcal{M}_{N,DN} - c = \mathcal{M}_{ND,ND} - c.$$

Remark 4.1 The operator $\mathcal{C}$ in (1.1) utilizes a 2D computational domain which is indicated by the integration variable $dx'dy' = d(x', y')$. We can show the construction of each operator by paying attention to the computational domain of each

operator and rearranging (4.3) using the agreement of operators in the bulk in the following way.

$$
\begin{aligned}
\mathcal{C} &= \mathcal{C} I_{x',y'} \\
&= \mathcal{X} I_{x'} \, \mathcal{Y} I_{y'} \\
&= \mathcal{X}(P_{e,x'} + P_{o,x'}) \, \mathcal{Y}(P_{e,y'} + P_{o,y'}) \\
&= (\mathcal{X} P_{e,x'} + \mathcal{X} P_{o,x'}) \, (\mathcal{Y} P_{e,y'} + \mathcal{Y} P_{o,y'}) \\
&= (\mathcal{X}_{\mathrm{p}} P_{e,x'} + \mathcal{X}_{\mathrm{a}} P_{o,x'}) \, (\mathcal{Y}_{\mathrm{p}} P_{e,y'} + \mathcal{Y}_{\mathrm{a}} P_{o,y'}) \quad =: -(\mathcal{M}_{\mathrm{N}} - c) \\
&= (\mathcal{X}_{\mathrm{a}} P_{e,x'} + \mathcal{X}_{\mathrm{p}} P_{o,x'}) \, (\mathcal{Y}_{\mathrm{a}} P_{e,y'} + \mathcal{Y}_{\mathrm{p}} P_{o,y'}) \quad =: -(\mathcal{M}_{\mathrm{D}} - c) \\
&= (\mathcal{X}_{\mathrm{p}} P_{e,x'} + \mathcal{X}_{\mathrm{a}} P_{o,x'}) \, (\mathcal{Y}_{\mathrm{ap}} P_{e,y'} + \mathcal{Y}_{\mathrm{pa}} P_{o,y'}) =: -(\mathcal{M}_{\mathrm{N,\,ND}} - c) \quad (4.17) \\
&= (\mathcal{X}_{\mathrm{ap}} P_{e,x'} + \mathcal{X}_{\mathrm{ap}} P_{o,x'})(\mathcal{Y}_{\mathrm{ap}} P_{e,y'} + \mathcal{Y}_{\mathrm{ap}} P_{o,y'}) =: -(\mathcal{M}_{\mathrm{ND,\,ND}} - c). \quad (4.18)
\end{aligned}
$$

We construct the operators in higher dimensions by using the corresponding rearrangement; see Section 7 for the 3D construction. In addition, the 2D decomposition operator $I_{x',y'}$ given in (2.6) is indeed the product of the 1D decomposition operators $I_{x'}$ and $I_{y'}$ given in (2.5). More precisely,

$$
\begin{aligned}
I_{x',y'} &= I_{x'} \, I_{y'} \\
&= (P_{e,x'} + P_{o,x'})(P_{e,y'} + P_{o,y'}) \\
&= P_{e,x'} P_{e,y'} + P_{e,x'} P_{o,y'} + P_{o,x'} P_{e,y'} + P_{o,x'} P_{o,y'}.
\end{aligned}
$$

5 Verifying the boundary conditions

We prove that the operators $\mathcal{M}_{\mathrm{N}}$, $\mathcal{M}_{\mathrm{D}}$, $\mathcal{M}_{\mathrm{ND,\,ND}}$, and $\mathcal{M}_{\mathrm{N,\,ND}}$ enforce pure Neumann, pure Dirichlet, mixed Neumann-Dirichlet (2+2), and mixed Neumann-Dirichlet (3+1) BC in 2D, respectively. Note that the operators $(\mathcal{M}_{\mathrm{N}} - c)$, $(\mathcal{M}_{\mathrm{D}} - c)$, $(\mathcal{M}_{\mathrm{N,\,DN}} - c)$, and $(\mathcal{M}_{\mathrm{ND,\,ND}} - c)$ given in (4.13), (4.14), (4.15), and (4.16), respectively, are the product of two 1D operators. As we mentioned, the limit in the definition of the BC can be interchanged with the integral sign due to the Lebesgue Dominated Convergence Theorem and the Leibniz Rule. Then, using the change in the order of integration as in (4.4), we prove that the pure Neumann and pure Dirichlet BC are enforced.

$$
\frac{\partial}{\partial n}\big[(\mathcal{M}_{\mathrm{N}} - c)u\big](x, +1) = -\Big(\frac{\partial}{\partial y}\mathcal{X}_{\mathrm{N}}\mathcal{Y}_{\mathrm{N}}\Big) u(x, +1) = -\mathcal{X}_{\mathrm{N}}\Big(\frac{d}{dy}\mathcal{Y}_{\mathrm{N}}\Big) u(x, +1) = 0
$$

$$
\frac{\partial}{\partial n}\big[(\mathcal{M}_{\mathrm{N}} - c)u\big](x, -1) = \Big(\frac{\partial}{\partial y}\mathcal{X}_{\mathrm{N}}\mathcal{Y}_{\mathrm{N}}\Big) u(x, -1) = \mathcal{X}_{\mathrm{N}}\Big(\frac{d}{dy}\mathcal{Y}_{\mathrm{N}}\Big) u(x, -1) = 0
$$

$$
\frac{\partial}{\partial n}\big[(\mathcal{M}_{\mathrm{N}} - c)u\big](+1, y) = -\Big(\frac{\partial}{\partial x}\mathcal{Y}_{\mathrm{N}}\mathcal{X}_{\mathrm{N}}\Big) u(+1, y) = -\mathcal{Y}_{\mathrm{N}}\Big(\frac{d}{dx}\mathcal{X}_{\mathrm{N}}\Big) u(+1, y) = 0
$$

$$
\frac{\partial}{\partial n}\big[(\mathcal{M}_{\mathrm{N}} - c)u\big](-1, y) = \Big(\frac{\partial}{\partial x}\mathcal{Y}_{\mathrm{N}}\mathcal{X}_{\mathrm{N}}\Big) u(-1, y) = \mathcal{Y}_{\mathrm{N}}\Big(\frac{d}{dx}\mathcal{X}_{\mathrm{N}}\Big) u(-1, y) = 0.
$$

$$
(\mathcal{M}_{\mathrm{D}} - c)u(x, \pm 1) = -\mathcal{X}_{\mathrm{D}}\mathcal{Y}_{\mathrm{D}}u(x, \pm 1) = 0
$$

$$
(\mathcal{M}_{\mathrm{D}} - c)u(\pm 1, y) = -\mathcal{Y}_{\mathrm{D}}\mathcal{X}_{\mathrm{D}}u(\pm 1, y) = 0.
$$

In addition, we prove that the operator $\mathcal{M}_{\text{N, DN}}$ enforces mixed Neumann-Dirichlet (3+1), i.e., the East, West, and North edges have Neumann and the South edge have Dirichlet BC.

$$\frac{\partial}{\partial n}\big[(\mathcal{M}_{\text{N, DN}} - c)u\big](+1, y) = -\left(\frac{\partial}{\partial x}\mathcal{Y}_{\text{DN}}\mathcal{X}_{\text{N}}\right)u(+1, y) = \mathcal{Y}_{\text{DN}}\left(\frac{d}{dx}\mathcal{X}_{\text{N}}\right)u(+1, y) = 0$$

$$\frac{\partial}{\partial n}\big[(\mathcal{M}_{\text{N, DN}} - c)u\big](-1, y) = \left(\frac{\partial}{\partial x}\mathcal{Y}_{\text{DN}}\mathcal{X}_{\text{N}}\right)u(-1, y) \ = \mathcal{Y}_{\text{DN}}\left(\frac{d}{dx}\mathcal{X}_{\text{N}}\right)u(-1, y) \ = 0$$

$$\frac{\partial}{\partial n}\big[(\mathcal{M}_{\text{N, DN}} - c)u\big](x, +1) = -\left(\frac{\partial}{\partial y}\mathcal{X}_{\text{N}}\mathcal{Y}_{\text{DN}}\right)u(x, +1) = -\mathcal{X}_{\text{N}}\left(\frac{d}{dy}\mathcal{Y}_{\text{DN}}\right)u(x, +1) = 0.$$

$$\big(\mathcal{M}_{\text{N, DN}} - c\big)u(x, -1) = -\mathcal{X}_{\text{N}}\mathcal{Y}_{\text{DN}}u(x, -1) = 0.$$

Finally, using (3.25), we prove that the operator $\mathcal{M}_{\text{ND, ND}}$ enforces mixed (2+2) Neumann-Dirichlet, i.e., the West and South edges have Neumann and the East and North edges have Dirichlet BC.

$$\frac{\partial}{\partial n}\big[(\mathcal{M}_{\text{ND, ND}} - c)u\big](-1, y) = \left(\frac{\partial}{\partial x}\mathcal{Y}_{\text{ND}}\mathcal{X}_{\text{ND}}\right)u(-1, y) = \mathcal{Y}_{\text{ND}}\left(\frac{d}{dx}\mathcal{X}_{\text{ND}}\right)u(-1, y) = 0$$

$$\frac{\partial}{\partial n}\big[(\mathcal{M}_{\text{ND, ND}} - c)u\big](x, -1) = \left(\frac{\partial}{\partial y}\mathcal{X}_{\text{ND}}\mathcal{Y}_{\text{ND}}\right)u(x, -1) = \mathcal{X}_{\text{ND}}\left(\frac{d}{dy}\mathcal{Y}_{\text{ND}}\right)u(x, -1) = 0.$$

$$\big(\mathcal{M}_{\text{ND, ND}} - c\big)u(+1, y) \ = -\mathcal{X}_{\text{ND}}\mathcal{Y}_{\text{ND}}u(+1, y) = 0$$

$$\big(\mathcal{M}_{\text{ND, ND}} - c\big)u(x, +1) \ = -\mathcal{X}_{\text{ND}}\mathcal{Y}_{\text{ND}}u(x, +1) = 0.$$

6 Other possible boundary conditions

We have 6 different types of BC, i.e., $\texttt{BC} \in \{\texttt{N, D, p, a, ND, DN}\}$. We construct the types of BC in 2D by taking the product of the BC prescribed for the x-edges with y-edges. Hence, we have 36 types of BC in 2D. We show the BC enforced on each edge using the notation

$$\big[\text{N D}\big] \times \begin{bmatrix} \text{N} \\ \text{D} \end{bmatrix},$$

which indicates the following BC configuration and corresponds to configuration number 34.

N (Neumann)	on the West edge,	$x = -1$,
D (Dirichlet)	on the East edge,	$x = +1$,
D (Dirichlet)	on the South edge,	$y = -1$,
N (Neumann)	on the North edge,	$y = +1$.

With pure BC both on the x- and y-edges we have 16 combinations; see Table 1. With pure BC on the x-edges and mixed on the y-edges, we have 8 combinations;

Table 1 The operators that enforce pure boundary conditions on each edge

No	BC	Operator		
1.	$[N\ N] \times \begin{bmatrix} N \\ N \end{bmatrix}$	$\mathcal{M}_N - c$	$= -(\mathcal{X}_p P_{e,x'} + \mathcal{X}_a P_{o,x'})$	$(\mathcal{Y}_p P_{e,y'} + \mathcal{Y}_a P_{o,y'})$
2.	$[N\ N] \times \begin{bmatrix} D \\ D \end{bmatrix}$	$\mathcal{M}_{N,D} - c$	$= -(\mathcal{X}_p P_{e,x'} + \mathcal{X}_a P_{o,x'})$	$(\mathcal{Y}_a P_{e,y'} + \mathcal{Y}_p P_{o,y'})$
3.	$[N\ N] \times \begin{bmatrix} p \\ p \end{bmatrix}$	$\mathcal{M}_{N,p} - c$	$= -(\mathcal{X}_p P_{e,x'} + \mathcal{X}_a P_{o,x'})$	$(\mathcal{Y}_p P_{e,y'} + \mathcal{Y}_p P_{o,y'})$
4.	$[N\ N] \times \begin{bmatrix} a \\ a \end{bmatrix}$	$\mathcal{M}_{N,a} - c$	$= -(\mathcal{X}_p P_{e,x'} + \mathcal{X}_a P_{o,x'})$	$(\mathcal{Y}_a P_{e,y'} + \mathcal{Y}_a P_{o,y'})$
5.	$[D\ D] \times \begin{bmatrix} N \\ N \end{bmatrix}$	$\mathcal{M}_{D,N} - c$	$= -(\mathcal{X}_a P_{e,x'} + \mathcal{X}_p P_{o,x'})$	$(\mathcal{Y}_p P_{e,y'} + \mathcal{Y}_a P_{o,y'})$
6.	$[D\ D] \times \begin{bmatrix} D \\ D \end{bmatrix}$	$\mathcal{M}_D - c$	$= -(\mathcal{X}_a P_{e,x'} + \mathcal{X}_p P_{o,x'})$	$(\mathcal{Y}_a P_{e,y'} + \mathcal{Y}_p P_{o,y'})$
7.	$[D\ D] \times \begin{bmatrix} p \\ p \end{bmatrix}$	$\mathcal{M}_{D,p} - c$	$= -(\mathcal{X}_a P_{e,x'} + \mathcal{X}_p P_{o,x'})$	$(\mathcal{Y}_p P_{e,y'} + \mathcal{Y}_p P_{o,y'})$
8.	$[D\ D] \times \begin{bmatrix} a \\ a \end{bmatrix}$	$\mathcal{M}_{D,a} - c$	$= -(\mathcal{X}_a P_{e,x'} + \mathcal{X}_p P_{o,x'})$	$(\mathcal{Y}_a P_{e,y'} + \mathcal{Y}_a P_{o,y'})$
9.	$[p\ p] \times \begin{bmatrix} N \\ N \end{bmatrix}$	$\mathcal{M}_{p,N} - c$	$= -(\mathcal{X}_p P_{e,x'} + \mathcal{X}_p P_{o,x'})$	$(\mathcal{Y}_p P_{e,y'} + \mathcal{Y}_a P_{o,y'})$
10.	$[p\ p] \times \begin{bmatrix} D \\ D \end{bmatrix}$	$\mathcal{M}_{p,D} - c$	$= -(\mathcal{X}_p P_{e,x'} + \mathcal{X}_p P_{o,x'})$	$(\mathcal{Y}_a P_{e,y'} + \mathcal{Y}_p P_{o,y'})$
11.	$[p\ p] \times \begin{bmatrix} p \\ p \end{bmatrix}$	$\mathcal{M}_p - c$	$= -(\mathcal{X}_p P_{e,x'} + \mathcal{X}_p P_{o,x'})$	$(\mathcal{Y}_p P_{e,y'} + \mathcal{Y}_p P_{o,y'})$
12.	$[p\ p] \times \begin{bmatrix} a \\ a \end{bmatrix}$	$\mathcal{M}_{p,a} - c$	$= -(\mathcal{X}_p P_{e,x'} + \mathcal{X}_p P_{o,x'})$	$(\mathcal{Y}_a P_{e,y'} + \mathcal{Y}_a P_{o,y'})$
13.	$[a\ a] \times \begin{bmatrix} N \\ N \end{bmatrix}$	$\mathcal{M}_{a,N} - c$	$= -(\mathcal{X}_a P_{e,x'} + \mathcal{X}_a P_{o,x'})$	$(\mathcal{Y}_p P_{e,y'} + \mathcal{Y}_a P_{o,y'})$
14.	$[a\ a] \times \begin{bmatrix} D \\ D \end{bmatrix}$	$\mathcal{M}_{a,D} - c$	$= -(\mathcal{X}_a P_{e,x'} + \mathcal{X}_a P_{o,x'})$	$(\mathcal{Y}_a P_{e,y'} + \mathcal{Y}_p P_{o,y'})$
15.	$[a\ a] \times \begin{bmatrix} p \\ p \end{bmatrix}$	$\mathcal{M}_{a,p} - c$	$= -(\mathcal{X}_a P_{e,x'} + \mathcal{X}_a P_{o,x'})$	$(\mathcal{Y}_p P_{e,y'} + \mathcal{Y}_p P_{o,y'})$
16.	$[a\ a] \times \begin{bmatrix} a \\ a \end{bmatrix}$	$\mathcal{M}_a - c$	$= -(\mathcal{X}_a P_{e,x'} + \mathcal{X}_a P_{o,x'})$	$(\mathcal{Y}_a P_{e,y'} + \mathcal{Y}_a P_{o,y'})$

see Table 2. With mixed BC on the x-edges and pure on the y-edges, we have 8 combinations; see Table 3. With mixed BC both on the x- and on the y-edges, we have 4 combinations; see Table 4.

Table 2 The operators that enforce pure boundary conditions on the x-edges and mixed boundary conditions on the y-edges

No	BC	Operator		
17.	$[\text{N N}] \times \begin{bmatrix} \text{D} \\ \text{N} \end{bmatrix}$	$\mathcal{M}_{\text{N, ND}} - c$	$= -(\mathcal{X}_p P_{e,x'} + \mathcal{X}_a P_{o,x'})$	$(\mathcal{Y}_{ap} P_{e,y'} + \mathcal{Y}_{pa} P_{o,y'})$
18.	$[\text{N N}] \times \begin{bmatrix} \text{N} \\ \text{D} \end{bmatrix}$	$\mathcal{M}_{\text{N, DN}} - c$	$= -(\mathcal{X}_p P_{e,x'} + \mathcal{X}_a P_{o,x'})$	$(\mathcal{Y}_{pa} P_{e,y'} + \mathcal{Y}_{ap} P_{o,y'})$
19.	$[\text{D D}] \times \begin{bmatrix} \text{D} \\ \text{N} \end{bmatrix}$	$\mathcal{M}_{\text{D, ND}} - c$	$= -(\mathcal{X}_a P_{e,x'} + \mathcal{X}_p P_{o,x'})$	$(\mathcal{Y}_{ap} P_{e,y'} + \mathcal{Y}_{pa} P_{o,y'})$
20.	$[\text{D D}] \times \begin{bmatrix} \text{N} \\ \text{D} \end{bmatrix}$	$\mathcal{M}_{\text{D, DN}} - c$	$= -(\mathcal{X}_a P_{e,x'} + \mathcal{X}_p P_{o,x'})$	$(\mathcal{Y}_{pa} P_{e,y'} + \mathcal{Y}_{ap} P_{o,y'})$
21.	$[\text{p p}] \times \begin{bmatrix} \text{D} \\ \text{N} \end{bmatrix}$	$\mathcal{M}_{\text{p, ND}} - c$	$= -(\mathcal{X}_p P_{e,x'} + \mathcal{X}_p P_{o,x'})$	$(\mathcal{Y}_{ap} P_{e,y'} + \mathcal{Y}_{pa} P_{o,y'})$
22.	$[\text{p p}] \times \begin{bmatrix} \text{N} \\ \text{D} \end{bmatrix}$	$\mathcal{M}_{\text{p, DN}} - c$	$= -(\mathcal{X}_p P_{e,x'} + \mathcal{X}_p P_{o,x'})$	$(\mathcal{Y}_{pa} P_{e,y'} + \mathcal{Y}_{ap} P_{o,y'})$
23.	$[\text{a a}] \times \begin{bmatrix} \text{D} \\ \text{N} \end{bmatrix}$	$\mathcal{M}_{\text{a, ND}} - c$	$= -(\mathcal{X}_a P_{e,x'} + \mathcal{X}_a P_{o,x'})$	$(\mathcal{Y}_{ap} P_{e,y'} + \mathcal{Y}_{pa} P_{o,y'})$
24.	$[\text{a a}] \times \begin{bmatrix} \text{N} \\ \text{D} \end{bmatrix}$	$\mathcal{M}_{\text{a, DN}} - c$	$= -(\mathcal{X}_a P_{e,x'} + \mathcal{X}_a P_{o,x'})$	$(\mathcal{Y}_{pa} P_{e,y'} + \mathcal{Y}_{ap} P_{o,y'})$

Table 3 The operators that enforce mixed boundary conditions on the x-edges and pure boundary conditions on the y-edges

No	BC	Operator		
25.	$[\text{N D}] \times \begin{bmatrix} \text{N} \\ \text{N} \end{bmatrix}$	$\mathcal{M}_{\text{ND, N}} - c$	$= -(\mathcal{X}_{ap} P_{e,x'} + \mathcal{X}_{pa} P_{o,x'})$	$(\mathcal{Y}_p P_{e,y'} + \mathcal{Y}_a P_{o,y'})$
26.	$[\text{D N}] \times \begin{bmatrix} \text{N} \\ \text{N} \end{bmatrix}$	$\mathcal{M}_{\text{DN, N}} - c$	$= -(\mathcal{X}_{pa} P_{e,x'} + \mathcal{X}_{ap} P_{o,x'})$	$(\mathcal{Y}_p P_{e,y'} + \mathcal{Y}_a P_{o,y'})$
27.	$[\text{N D}] \times \begin{bmatrix} \text{D} \\ \text{D} \end{bmatrix}$	$\mathcal{M}_{\text{ND, D}} - c$	$= -(\mathcal{X}_{ap} P_{e,x'} + \mathcal{X}_{pa} P_{o,x'})$	$(\mathcal{Y}_a P_{e,y'} + \mathcal{Y}_p P_{o,y'})$
28.	$[\text{D N}] \times \begin{bmatrix} \text{D} \\ \text{D} \end{bmatrix}$	$\mathcal{M}_{\text{DN, D}} - c$	$= -(\mathcal{X}_{pa} P_{e,x'} + \mathcal{X}_{ap} P_{o,x'})$	$(\mathcal{Y}_a P_{e,y'} + \mathcal{Y}_p P_{o,y'})$
29.	$[\text{N D}] \times \begin{bmatrix} \text{p} \\ \text{p} \end{bmatrix}$	$\mathcal{M}_{\text{ND, p}} - c$	$= -(\mathcal{X}_{ap} P_{e,x'} + \mathcal{X}_{pa} P_{o,x'})$	$(\mathcal{Y}_p P_{e,y'} + \mathcal{Y}_p P_{o,y'})$
30.	$[\text{D N}] \times \begin{bmatrix} \text{p} \\ \text{p} \end{bmatrix}$	$\mathcal{M}_{\text{DN, p}} - c$	$= -(\mathcal{X}_{pa} P_{e,x'} + \mathcal{X}_{ap} P_{o,x'})$	$(\mathcal{Y}_p P_{e,y'} + \mathcal{Y}_p P_{o,y'})$
31.	$[\text{N D}] \times \begin{bmatrix} \text{a} \\ \text{a} \end{bmatrix}$	$\mathcal{M}_{\text{ND, a}} - c$	$= -(\mathcal{X}_{ap} P_{e,x'} + \mathcal{X}_{pa} P_{o,x'})$	$(\mathcal{Y}_a P_{e,y'} + \mathcal{Y}_a P_{o,y'})$
32.	$[\text{D N}] \times \begin{bmatrix} \text{a} \\ \text{a} \end{bmatrix}$	$\mathcal{M}_{\text{DN, a}} - c$	$= -(\mathcal{X}_{pa} P_{e,x'} + \mathcal{X}_{ap} P_{o,x'})$	$(\mathcal{Y}_a P_{e,y'} + \mathcal{Y}_a P_{o,y'})$

Table 4 The operators that enforce mixed boundary conditions on the x-edges and mixed boundary conditions on the y-edges

No	BC	Operator		
33.	$\begin{bmatrix} N\ D \end{bmatrix} \times \begin{bmatrix} D \\ N \end{bmatrix}$	$\mathcal{M}_{\text{ND, ND}} - c$	$= -\left(\mathcal{X}_{\text{ap}} P_{e,x'} + \mathcal{X}_{\text{pa}} P_{o,x'}\right)$	$\left(\mathcal{Y}_{\text{ap}} P_{e,y'} + \mathcal{Y}_{\text{pa}} P_{o,y'}\right)$
34.	$\begin{bmatrix} N\ D \end{bmatrix} \times \begin{bmatrix} N \\ D \end{bmatrix}$	$\mathcal{M}_{\text{ND, DN}} - c$	$= -\left(\mathcal{X}_{\text{ap}} P_{e,x'} + \mathcal{X}_{\text{pa}} P_{o,x'}\right)$	$\left(\mathcal{Y}_{\text{pa}} P_{e,y'} + \mathcal{Y}_{\text{ap}} P_{o,y'}\right)$
35.	$\begin{bmatrix} D\ N \end{bmatrix} \times \begin{bmatrix} D \\ N \end{bmatrix}$	$\mathcal{M}_{\text{DN, ND}} - c$	$= -\left(\mathcal{X}_{\text{pa}} P_{e,x'} + \mathcal{X}_{\text{ap}} P_{o,x'}\right)$	$\left(\mathcal{Y}_{\text{ap}} P_{e,y'} + \mathcal{Y}_{\text{pa}} P_{o,y'}\right)$
36.	$\begin{bmatrix} D\ N \end{bmatrix} \times \begin{bmatrix} N \\ D \end{bmatrix}$	$\mathcal{M}_{\text{DN, DN}} - c$	$= -\left(\mathcal{X}_{\text{pa}} P_{e,x'} + \mathcal{X}_{\text{ap}} P_{o,x'}\right)$	$\left(\mathcal{Y}_{\text{pa}} P_{e,y'} + \mathcal{Y}_{\text{ap}} P_{o,y'}\right)$

7 Operators in higher dimensions

Let us consider the convolution in 3D and the domain be $\Omega := (-1, 1) \times (-1, 1) \times (-1, 1)$. We define the convolution in 3D similarly using notation in (4.2).

$$\mathcal{C}u(x, y) = \iiint_{\Omega} \widehat{C}(x'-x, y'-y, z'-z)u(x', y', z')dx'dy'dz'.$$

Note that $\mathcal{C} = -(\mathcal{L} - c)$. Hence we concentrate on finding suitable operators that agree with $\mathcal{C}$ in the bulk. Assuming a separable kernel function similar to (2.7),

$$C(x, y, z) = X(x)Y(y)Z(z),$$

the operators $\mathcal{M}_{\text{N}}$ and $\mathcal{M}_{\text{D}}$ in 3D defined below enforce pure Neumann and Dirichlet BC and simultaneously agree with the operator $\mathcal{L}$ in the bulk. The construction process is an extension of the 2D case.

$$
\begin{aligned}
\mathcal{C} &= \mathcal{C}I_{x',y',z'} \\
&= \mathcal{X}I_{x'}\,\mathcal{Y}I_{y'}\,\mathcal{Z}I_{z'} \\
&= \mathcal{X}(P_{e,x'} + P_{o,x'})\,\mathcal{Y}(P_{e,y'} + P_{o,y'})\,\mathcal{Z}(P_{e,z'} + P_{o,z'}) \\
&= \left(\mathcal{X}P_{e,x'} + \mathcal{X}P_{o,x'}\right)\left(\mathcal{Y}P_{e,y'} + \mathcal{Y}P_{o,y'}\right)\left(\mathcal{Z}P_{e,z'} + \mathcal{Z}P_{o,z'}\right) \\
&= \left(\mathcal{X}_{\text{p}}P_{e,x'} + \mathcal{X}_{\text{a}}P_{o,x'}\right)\left(\mathcal{Y}_{\text{p}}P_{e,y'} + \mathcal{Y}_{\text{a}}P_{o,y'}\right)\left(\mathcal{Z}_{\text{p}}P_{e,z'} + \mathcal{Z}_{\text{a}}P_{o,z'}\right) =: -(\mathcal{M}_{\text{N}}-c) \\
&= \left(\mathcal{X}_{\text{a}}P_{e,x'} + \mathcal{X}_{\text{p}}P_{o,x'}\right)\left(\mathcal{Y}_{\text{a}}P_{e,y'} + \mathcal{Y}_{\text{p}}P_{o,y'}\right)\left(\mathcal{Z}_{\text{a}}P_{e,y'} + \mathcal{Z}_{\text{p}}P_{o,z'}\right) =: -(\mathcal{M}_{\text{D}}-c).
\end{aligned}
$$

The operators that enforce mixed Neumann and Dirichlet BC can be constructed in a similar fashion to the operators given in (4.18) and (4.17). The extension to arbitrary dimension can be performed by the same line of argument.

8 Numerical experiments

8.1 Nonlocal wave equation

We numerically solve the following nonlocal wave equation

$$u_{tt}(x, y, t) + \mathcal{M}_{\text{BC}}u(x, y, t) = b(x, y, t), \quad (x, y, t) \in \Omega \times J, \quad (8.1a)$$
$$u(x, y, 0) = u_0(x, y), \quad (x, y) \in \Omega, \quad (8.1b)$$
$$u_t(x, y, 0) = v_0(x, y), \quad (x, y) \in \Omega, \quad (8.1c)$$

where $J = (0, T)$ is some finite time interval, $\Omega = (-1, 1) \times (-1, 1)$, b is a given source term, and u_0 and v_0 are given initial displacement and velocity of the wave equation, respectively. The choice of the subscript BC is determined by the BC that are to be satisfied at the boundary of the physical domain Ω. Approximate solutions of the nonlocal wave equation (8.1) were obtained by the numerical scheme which is described below.

8.1.1 Discretization in space

To approximate the solution of (8.1), we begin with discretizing the domain Ω by introducing the grid

$$\{(x_i, y_j) : 0 \leq i \leq N_x, \ 0 \leq j \leq N_y\}$$

where

$$-1 = x_0 < x_1 < \cdots < x_{N_x-1} < x_{N_x} = 1$$

and

$$-1 = y_0 < y_1 < \cdots < y_{N_y-1} < y_{N_y} = 1.$$

Although it is possible to take different values for N_x and N_y, for the sake of simplicity of the presentation we take $N_x = N_y = N$. Furthermore, we assume that the grid spacing in both dimensions is uniform, that is,

$$x_i - x_{i-1} = y_j - y_{j-1} =: h = \frac{2}{N} \quad \text{for all } i = 1, \ldots, N \text{ and } j = 1, \ldots, N.$$

Note, however, that it is possible to remove either of these assumptions without much difficulty.

We would like to compute an approximation u^h to the solution u of (8.1) at the grid points $\{(x_i, y_i) : i = 1, \ldots, N\}$ by employing a collocation method which is obtained by requiring that the equation (8.1) holds true at all grid points, i.e.,

$$u_{tt}^h(x_i, y_i, t) + \mathcal{M}_{\text{BC}}u^h(x_i, y_i, t) = b(x_i, y_i, t),$$
$$u^h(x_i, y_i, 0) = u_0(x_i, y_i),$$
$$u_t^h(x_i, y_i, 0) = v_0(x_i, y_i), \quad (8.2)$$

for all $i = 1, \ldots, N$ and $t \in J$. The integrals in $\mathcal{M}_{\text{BC}}$ are to be approximated by a trapezoidal rule. Our collocation method of choice is the Nyström method which

is obtained when the nodes of the trapezoidal rule for numerical integration are also chosen as the grid points.

8.1.2 Discretization in time

The discretization of (8.1) by the Nyström method (8.2) leads to the second-order system of ordinary differential equations

$$\ddot{\mathbf{u}}^h(t) + \mathbf{A}\mathbf{u}^h(t) = \mathbf{b}^h(t), \qquad t \in J,$$
$$\mathbf{u}^h(0) = \mathbf{u}_0^h,$$
$$\dot{\mathbf{u}}^h(0) = \mathbf{v}_0^h. \tag{8.3}$$

Here, $\mathbf{A}$ denotes the stiffness matrix. To discretize (8.3) in time, we employ the Newmark time-stepping scheme as described in [19]. Let Δt denote the time step and set $t_n = n \cdot \Delta t$ for $n = 1, 2, \ldots$. The Newmark scheme we employ consists of finding approximations $\{\mathbf{u}_n^h\}_n$ to $\mathbf{u}^h(t_n)$ such that

$$\mathbf{u}_1^h = \big(\mathbf{I} - \frac{1}{2}\Delta t^2 \mathbf{A}\big)\mathbf{u}_0^h + \Delta t \mathbf{v}_0^h + \frac{1}{2}\Delta t^2 \mathbf{b}_0^h,$$
$$\mathbf{u}_{n+1}^h = \big(2\mathbf{I} - \Delta t^2 \mathbf{A}\big)\mathbf{u}_n^h - \mathbf{u}_{n-1}^h + \Delta t^2 \mathbf{b}_n^h,$$

for $n = 1, 2, \ldots, N_t - 1$ where $N_t \Delta t = T$, and $\mathbf{b}_n^h = \mathbf{b}^h(t_n)$. Although there is a more general version of the Newmark time-stepping schemes, we made this particular choice due to the fact that it is explicit and second-order accurate. For a detailed discussion, we refer to [19].

8.1.3 Approximations to explicitly known exact solutions

In order to ascertain the convergence performance of the numerical scheme described above, we display some numerical results corresponding to explicitly known exact solutions. We solve one example corresponding to four of the BC types described in Tables 1, 2, 3, and 4. More explicitly, No. 1 and 6 in Table 1, No. 17 in Table 2, and No. 33 in Table 4. We take the exact solution corresponding to each BC as given in Table 5 and compute the corresponding right-hand side function $b(x, y, t)$. We then compute the approximate solution by the Nyström method as described above. For the simplicity of being able to compute the right-hand side function $b(x, y, t)$ for a given exact solution $u(x, y, t)$, we take the kernel function C to be identically equal to 1 on Ω. However, this is by no means a requirement for actual numerical computations. For implementation, we use the explicit expression of the kernel functions associated with the operators $\mathcal{M}_{\mathrm{N}}$, $\mathcal{M}_{\mathrm{D}}$, $\mathcal{M}_{\mathrm{N, DN}}$, and $\mathcal{M}_{\mathrm{ND, ND}}$ given by

$$\big(\mathcal{M}_{\mathrm{BC}} - c\big)u(x, y) = -\iint\limits_{\Omega} K_{\mathrm{BC}}(x, x', y, y')u(x', y')dx'dy',$$

Table 5 Known exact solutions used in numerical experiments

BC	$u(x, y, t)$
N	$t^2[(x + 1)^2(x - 1)^3(y + 1)^3(y - 1)^2 + 64/225]$
D	$t^2(x^2 - 1)(y^2 - 1)$
N, DN	$t^2(x + 1)^2(x - 1)^2(y + 1)(y - 1)^2$
ND, ND	$t^2(x + 1)^2(x - 1)(y + 1)^2(y - 1)$

where $\mathrm{BC} \in \{\mathrm{N}, \mathrm{D}, (\mathrm{N}, \mathrm{DN}), (\mathrm{ND}, \mathrm{ND})\}$ and

$$
K_{\mathrm{N}}(x, x', y, y') := \frac{1}{4}\big[\widehat{X}_{\mathrm{p}}(x'-x) + \widehat{X}_{\mathrm{p}}(x'+x) + \widehat{X}_{\mathrm{a}}(x'-x) - \widehat{X}_{\mathrm{a}}(x'+x)\big]
$$
$$
\big[\widehat{Y}_{\mathrm{p}}(y'-y) + \widehat{Y}_{\mathrm{p}}(y'+y) + \widehat{Y}_{\mathrm{a}}(y'-y) - \widehat{Y}_{\mathrm{a}}(y'+y)\big],
$$
$$
K_{\mathrm{D}}(x, x', y, y') := \frac{1}{4}\big[\widehat{X}_{\mathrm{a}}(x'-x) + \widehat{X}_{\mathrm{a}}(x'+x) + \widehat{X}_{\mathrm{p}}(x'-x) - \widehat{X}_{\mathrm{p}}(x'+x)\big]
$$
$$
\big[\widehat{Y}_{\mathrm{a}}(y'-y) + \widehat{Y}_{\mathrm{a}}(y'+y) + \widehat{Y}_{\mathrm{p}}(y'-y) - \widehat{Y}_{\mathrm{p}}(y'+y)\big],
$$
$$
K_{\mathrm{N}, \mathrm{DN}}(x, x', y, y') := \frac{1}{4}\big[\widehat{X}_{\mathrm{p}}(x'-x) + \widehat{X}_{\mathrm{p}}(x'+x) + \widehat{X}_{\mathrm{a}}(x'-x) - \widehat{X}_{\mathrm{a}}(x'+x)\big]
$$
$$
\big[\widehat{Y}_{\mathrm{ap}}(y'-y) + \widehat{Y}_{\mathrm{ap}}(y'+y) + \widehat{Y}_{\mathrm{pa}}(y'-y) - \widehat{Y}_{\mathrm{pa}}(y'+y)\big],
$$
$$
K_{\mathrm{ND}, \mathrm{ND}}(x, x', y, y') := \frac{1}{4}\big[\widehat{X}_{\mathrm{pa}}(x'-x) + \widehat{X}_{\mathrm{pa}}(x'+x) + \widehat{X}_{\mathrm{ap}}(x'-x) - \widehat{X}_{\mathrm{ap}}(x'+x)\big]
$$
$$
\big[\widehat{Y}_{\mathrm{pa}}(y'-y) + \widehat{Y}_{\mathrm{pa}}(y'+y) + \widehat{Y}_{\mathrm{ap}}(y'-y) - \widehat{Y}_{\mathrm{ap}}(y'+y)\big].
$$

For each problem, we compute the exact solution until the final time $T = 10$ and compute the relative discrete L^∞-error $\big\|(u - u^h)(\cdot, T)\big\|_{h,\infty} / \|u(\cdot, T)\|_{h,\infty}$ where

$$
\|\varphi\|_{h,\infty} := \max_{1 \le i \le N} |\varphi(x_i, y_i)|.
$$

We compute approximate solutions with uniform grids with $N = 2^i$ with $i = 2, \ldots, 6$. In each case, as the time step of the Newmark scheme, we take $\Delta t = 2^{-5}/10$ so that the explicit Newmark time integration scheme is stable. In all of our examples, we found out that taking Δt so that $\Delta t < h/10$ is sufficient for stability.

Table 6 History of convergence with known exact solutions

Grid	N		D		N,DN		ND,ND	
	Error	Rate	Error	Rate	Error	Rate	Error	Rate
2	2.68E-01	–	3.24E-01	–	3.55E-01	0.01	3.88E-01	–
3	9.59E-02	1.48	1.57E-01	1.05	2.15E-01	0.72	2.07E-01	0.90
4	4.83E-02	0.99	7.19E-02	1.13	1.09E-01	0.98	1.02E-01	1.03
5	2.47E-02	0.97	3.45E-02	1.06	5.39E-02	1.01	5.00E-02	1.02
6	1.26E-02	0.97	1.68E-02	1.03	2.68E-02	1.01	2.48E-02	1.01

Note that since the Newmark scheme is second order accurate in time, and all of the exact solutions in Table 5 is of the form $u(x, y, t) = T(t)U(x, y)$ with $T(t) = t^2$, a second order polynomial, it is guaranteed that the dominant error is the spatial one.

We display our numerical results in Table 6. Therein, the column labeled "grid" we display $\log_2 N$ and the column labeled "rate" displays the relative error corresponding to the approximate solution with that particular grid. In the column labeled "rate," we display an approximate rate of convergence as follows. If e_i denotes the relative error with the grid with $N = 2^i$, then we display the quantity

$$r_{i+1} = -\frac{1}{\log 2} \log\left(\frac{e_{i+1}}{e_i}\right)$$

at the row corresponding to grid$= i + 1$. The results displayed in Table 6 suggest an error estimate of the form

$$\frac{\left\|(u - u^h)(\cdot, T)\right\|_{h,\infty}}{\|u(\cdot, T)\|_{h,\infty}} \leq D h.$$

for some constant D independent of u and h, that is, the method converges with rate 1 with respect to h.

8.1.4 Approximations to unknown solutions

Here, we display some numerical results in which we solve (8.2) with $b = 0$. In this case, we do not have an explicit representation of the solution and merely rely on numerical computing. We consider two initial displacement functions

$$u_{0,\text{cont}}(x, y) = e^{x-3y+x^2y} \sin(xy)(1 - x^2)^2(1 - y^2)^3,$$

and

$$u_{0,\text{disc}}(x, y) = \begin{cases} 1, & (x, y) \in (-1/4, 1/4) \times (-1/4, 1/4), \\ 0, & \text{otherwise.} \end{cases}$$
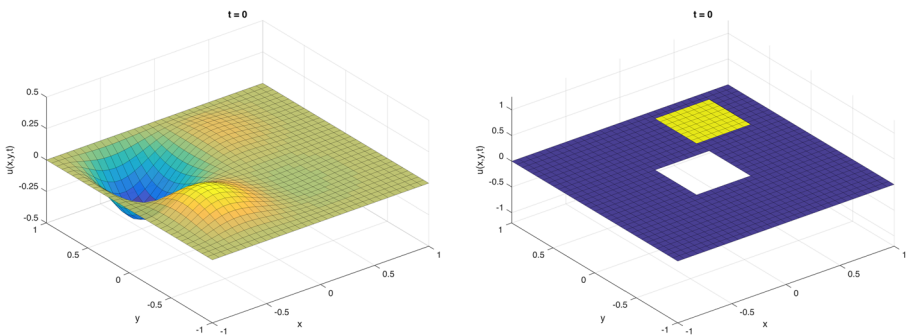
Fig. 3 Initial data to the nonlocal wave equation on a 2D domain with continuous (left) and discontinuous (right) initial data

These functions are displayed in Fig. 3. In all cases, the initial velocity $v_0(x, y) = 0$ for all $(x, y) \in \Omega$. The kernel function is taken to be

$$C(x, y) = \begin{cases} 1, & (x, y) \in (-\delta, \delta) \times (-\delta, \delta), \\ 0, & \text{otherwise.} \end{cases} \tag{8.4}$$
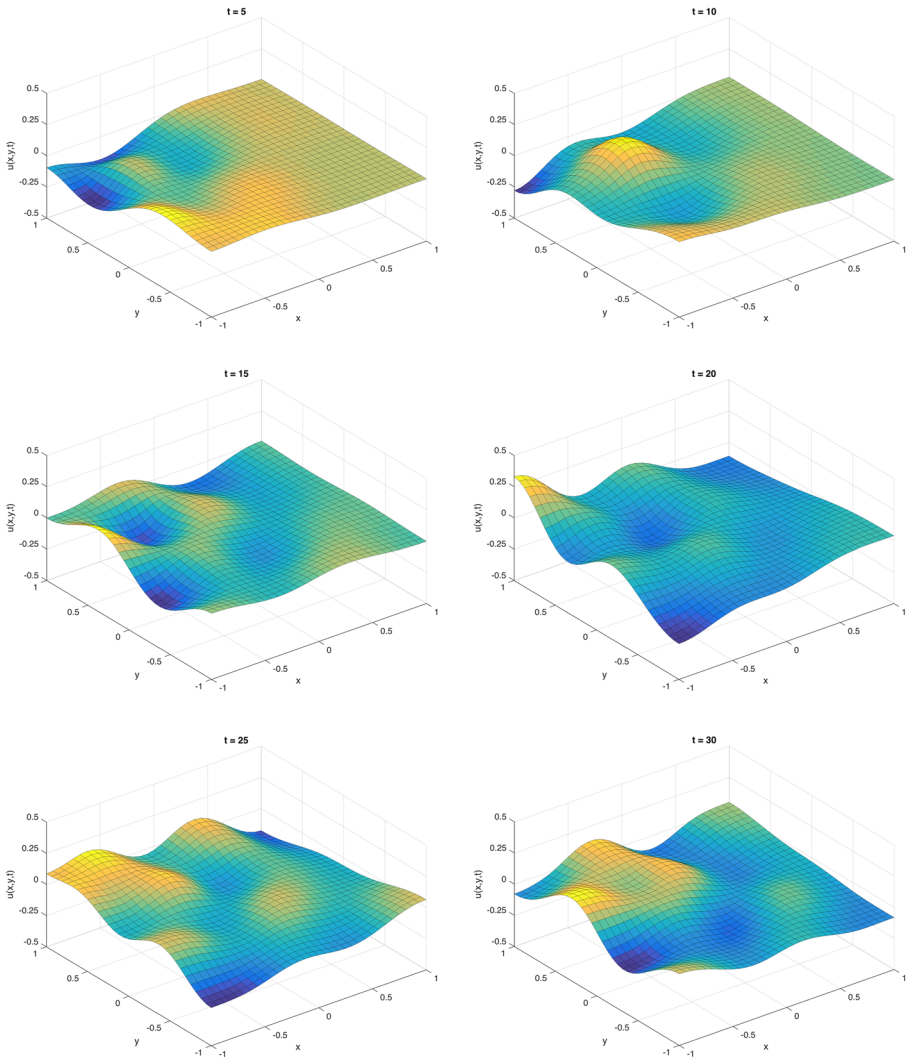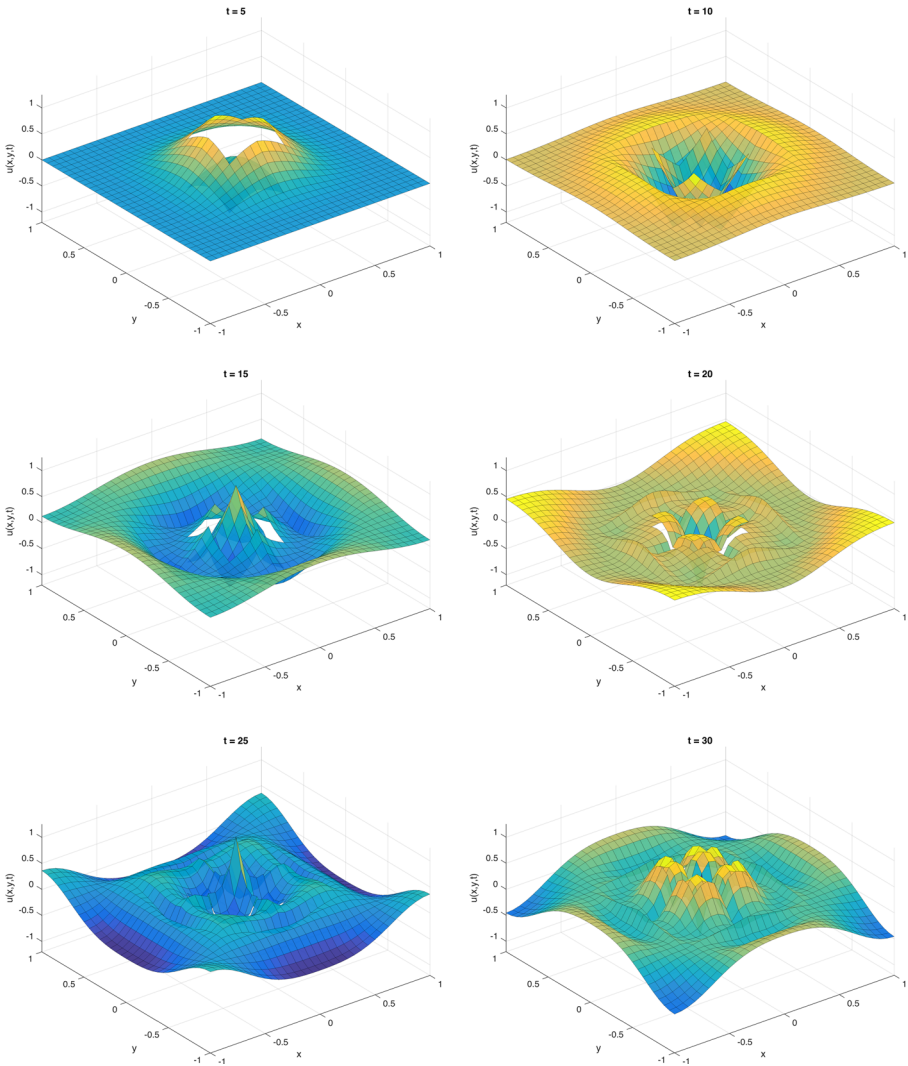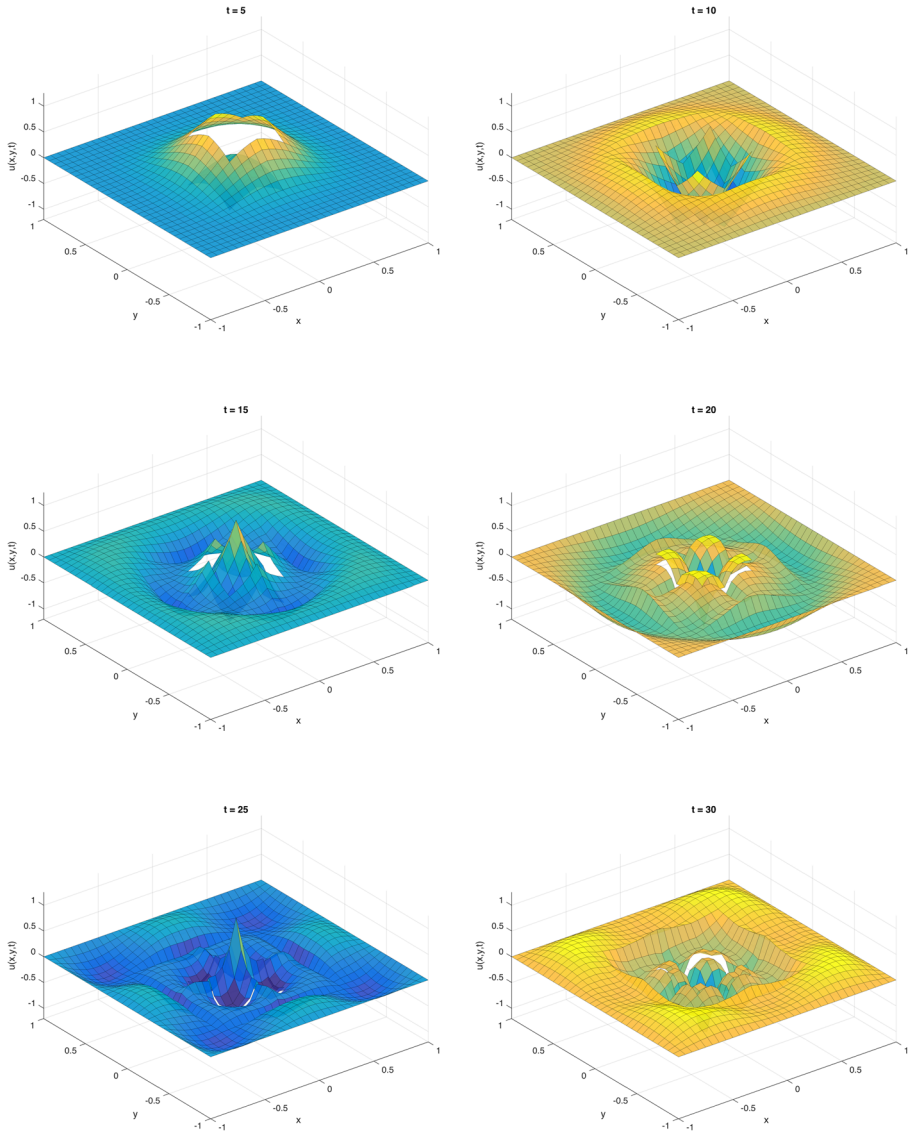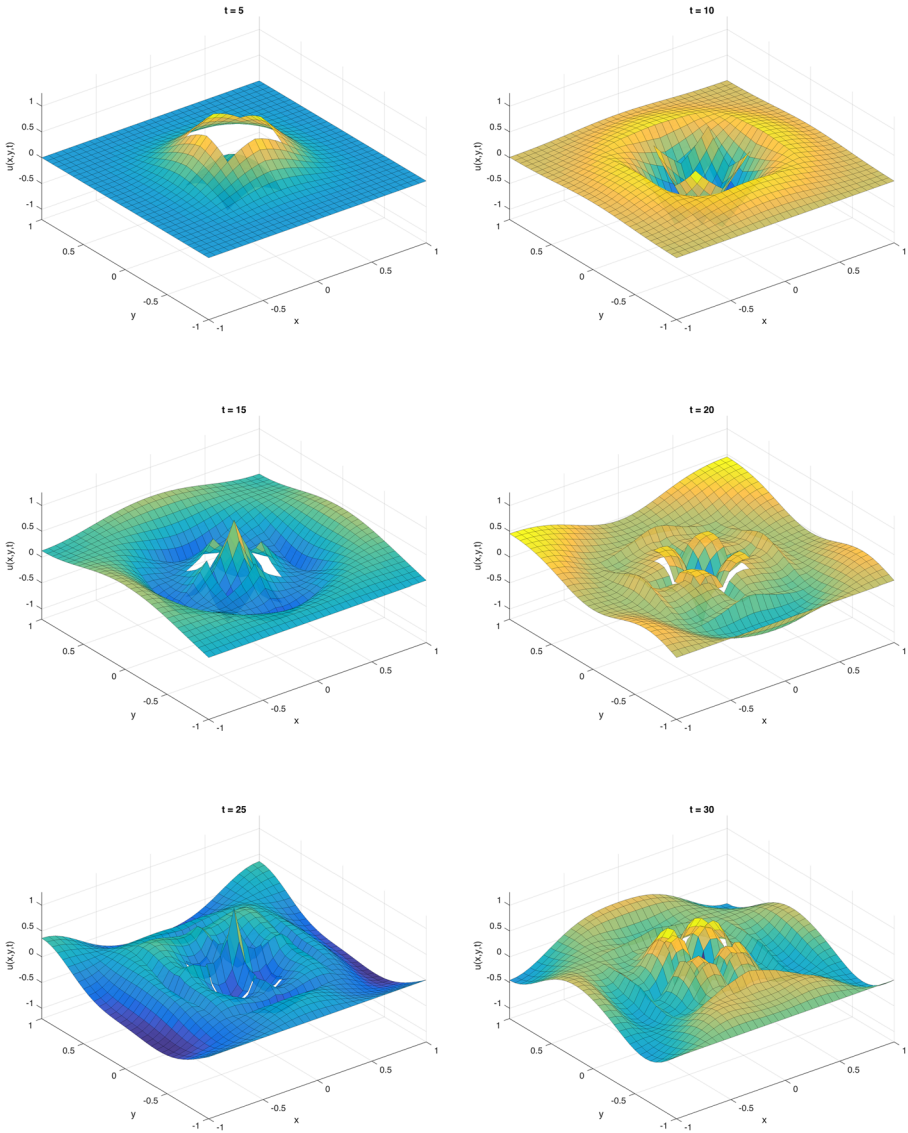

Fig. 4 Solution to the nonlocal wave equation on a 2D domain with continuous initial data using the operator $\mathcal{M}_{\mathrm{N}}$ which corresponds to the boundary condition configuration 1

In all examples, we use a grid with $N = 32$ and take the horizon $\delta = 2^{-2}$. We display results for the continuous initial displacement only for $\text{BC} = \text{N}$ which is depicted in Fig. 4. For the discontinuous initial displacement we display the approximate solution for $\text{BC} \in \{\text{N}, \text{D}, (\text{N}, \text{DN}), (\text{ND}, \text{ND})\}$ in Figs. 5, 6, 7, and 8.

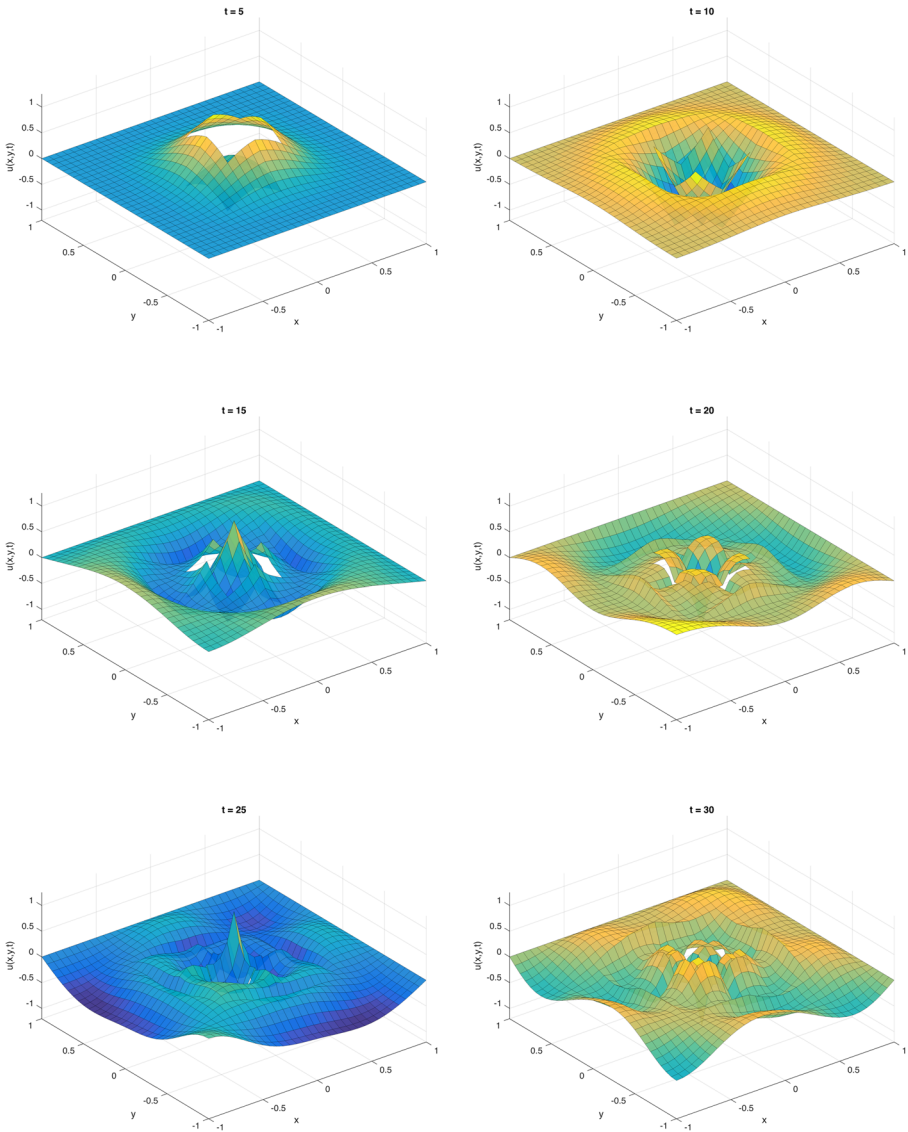**Fig. 5** Solution to the nonlocal wave equation on a 2D domain with discontinuous initial data using the operator $\mathcal{M}_\text{N}$ which corresponds to the boundary condition configuration 1

Fig. 6 Solution to the nonlocal wave equation on a 2D domain with discontinuous initial data using the operator $\mathcal{M}_\mathrm{D}$ which corresponds to the boundary condition configuration 6

In [2], for 1D problem and $t \in \mathbb{R}$, we have proved that the solution is discontinuous if and only if the initial data is discontinuous. Furthermore, the position of discontinuity is determined by the initial data and should remain stationary. We observe the similar behavior in 2D as well. The discontinuity located along the edges of the square $(-1/4, 1/4) \times (-1/4, 1/4)$ remains stationary.

Fig. 7 Solution to the nonlocal wave equation on a 2D domain with discontinuous initial data using the operator $\mathcal{M}_{\text{N, DN}}$ which corresponds to the boundary condition configuration 18

8.2 Comparison of solutions of the classical and nonlocal wave equations

We compare the solutions of the nonlocal wave equation (8.1) to that of the classical wave equation

$$u_{tt}(x, y, t) - c^2 \Delta u(x, y, t) = b(x, y, t), \quad (x, y, t) \in \Omega \times J, \tag{8.5a}$$

$$u(\pm 1, y, t) = u(x, \pm 1, t) = 0 \tag{8.5b}$$

with initial conditions (8.1b) and (8.1c). Here, c denotes the wave speed.

In 1D, for discontinuous initial data, the solution to the classical equation is obtained by d'Alembert's method. On the other hand, the solution to the nonlocal equation is obtained by the procedure described in [1]. For both solutions, we choose the initial data

$$u_{0,\text{disc}}(x) = \begin{cases} 1, & x \in (-1/16, 1/16), \\ 0, & \text{otherwise.} \end{cases}$$

Fig. 8 Solution to the nonlocal wave equation on a 2D domain with discontinuous initial data using the operator $\mathcal{M}_{\text{ND, ND}}$ which corresponds to the boundary condition configuration 33

The two solutions are depicted in Fig. 9 and they clearly disagree. The disagreement is more striking in the way the discontinuities propagate. They propagate along characteristics in the classical solution, whereas in the nonlocal solution, the position of discontinuity is determined by the initial data and remain stationary. The two solutions have similar wave separation and boundary reflection behavior. Namely, the Dirichlet BC create reflections of the opposite sign. The other striking difference is the dispersive behavior that the nonlocal solution exhibits.

In 2D, for continuous initial data, we employ the truncated series to approximate solutions of the classical wave equation (8.5a) given in the form

$$u(x, y, t) = \sum_{m=1}^{M} \sum_{n=1}^{N} a_{mn} \cos(\pi \sqrt{m^2 + n^2}\, ct) \sin\left(\frac{m\pi}{2}(x+1)\right) \sin\left(\frac{n\pi}{2}(y+1)\right)$$

(8.6)
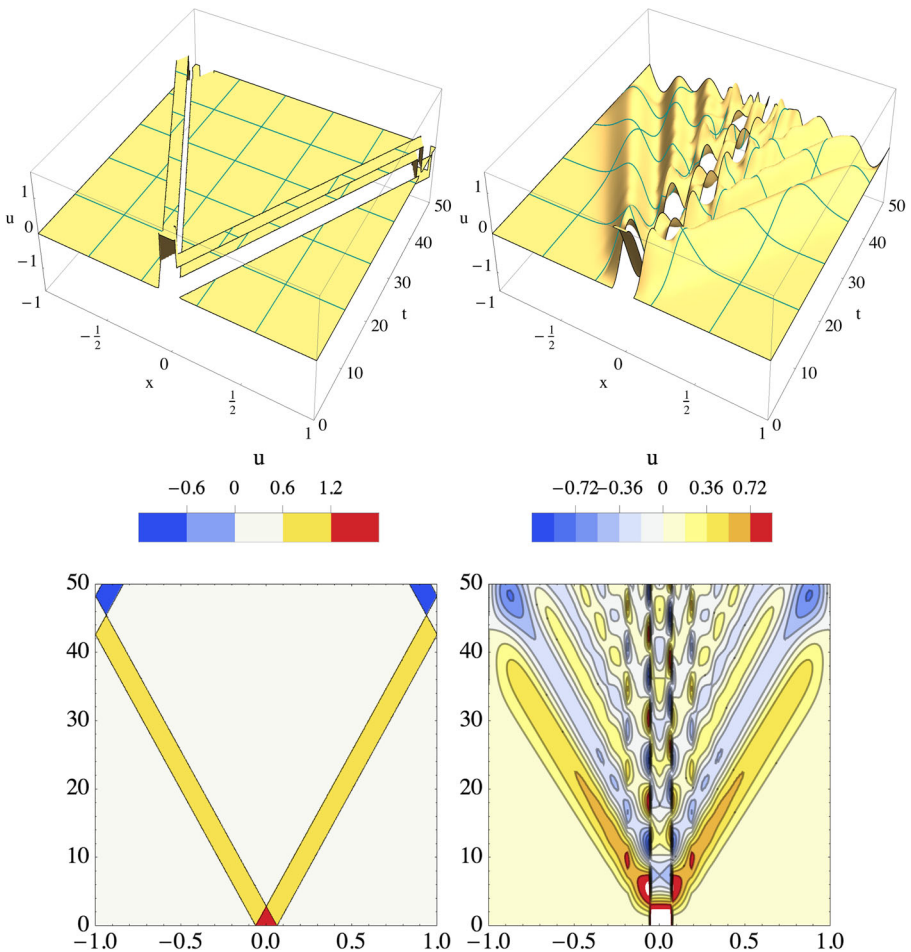
Fig. 9 Solutions to the classical (top left) and nonlocal (top right) wave equations on a 1D domain with identical discontinuous initial displacement. The corresponding contour plots are given in the bottom row
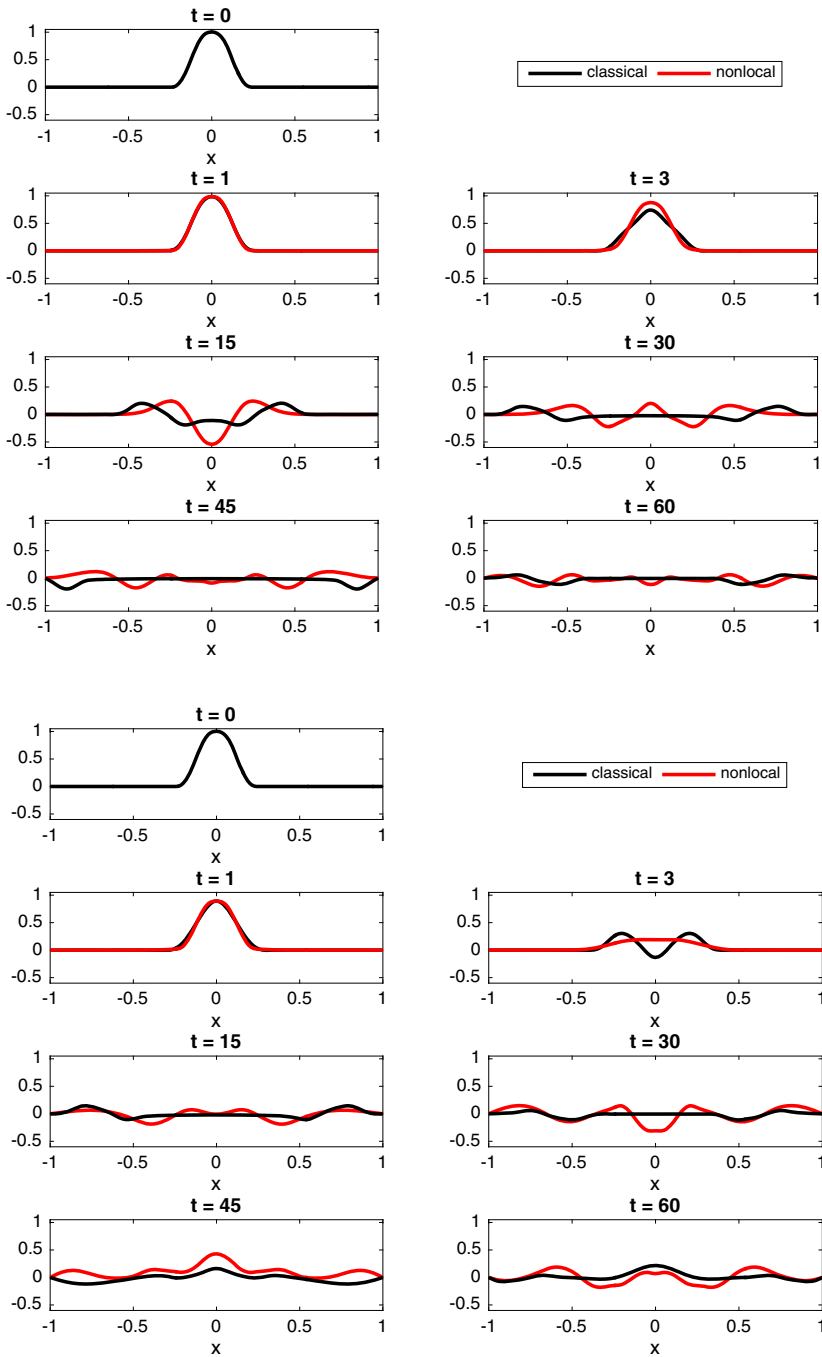
Fig. 10 Solutions $u(x, 0, t)$ to the 2D classical and nonlocal wave equations with continuous initial data. Top: $c = 0.011423$ and $\delta = 2^{-3}$. Bottom: $c = 0.02371$ and $\delta = 2^{-2}$. Note that larger horizon leads to more dispersion

where

$$a_{mn} = \int_{-1}^{1} \int_{-1}^{1} u_0(x, y) \sin\left(\frac{m\pi}{2}(x + 1)\right) \sin\left(\frac{n\pi}{2}(y + 1)\right) dy dx, \qquad (8.7)$$

and the initial displacement $u_0(x, y)$ is given in (8.1b) and the initial velocity $v_0(x, y)$ in (8.1c) is chosen to be 0.

We depict the solutions of the classical and nonlocal wave equations at the cross section $y = 0$ for various t. The diffusivity coefficient α is determined by requiring that the classical and nonlocal solutions coincide at $(x, y, t) = (0, 0, 1)$. In Fig. 10, we choose the horizon as $\delta = 2^{-3}$ and $\delta = 2^{-2}$ in the kernel function (8.4), and set $c = 0.011423$ and $c = 0.02371$, respectively, to obtain the corresponding classical solutions. In both figures, $u_{0,\text{cont}}(x, y) = u_{0,\text{cont}}(x)u_{0,\text{cont}}(y)$ where

$$u_{0,\text{cont}}(x) = \begin{cases} 0, & x \in (-1, -1/4), \\ (1 + 4x)^3(96x^2 - 12x + 1), & x \in [-1/4, 0), \\ (1 - 4x)^3(96x^2 + 12x + 1), & x \in [0, 1/4], \\ 0, & x \in (1/4, 1). \end{cases} \qquad (8.8)$$

The fact that (8.6) converges as $M, N \to \infty$ implies that $\lim_{m,n\to\infty} |a_{mn}| = 0$. For the initial data given in (8.8), we take $M = N = 35$, so that $|a_{MN}| \leq 10^{-6}$.

The two solutions share common features such as wave separation and a similar boundary reflection behavior. However, the nonlocal solution exhibits dispersive behavior which seems to be the major source of disagreement. That is why, when a larger horizon, i.e., $\delta = 2^{-2}$, is used, the disagreement is more pronounced than the case of $\delta = 2^{-3}$ due to more dispersion; cf. Fig. 10.

8.3 Nonlocal heat equation

We numerically solve the nonlocal heat equation

$$u_t(x, y, t) + \mathcal{M}_{\text{BC}}u(x, y, t) = b(x, y, t), \qquad (x, y, t) \in \Omega \times J, \qquad (8.9a)$$
$$u(x, y, 0) = u_0(x, y), \qquad (x, y) \in \Omega. \qquad (8.9b)$$

We choose the kernel function

$$C(x, y) = \begin{cases} \dfrac{1}{|x||y|}, & (x, y) \in (-\delta, \delta) \times (-\delta, \delta), \\ 0, & \text{otherwise,} \end{cases}$$

inspired by [13, 14], also see [25]. The spatial discretization is identical to the one given in Section 8.1.1. It leads to the first-order system of ordinary differential equations

$$\dot{\mathbf{u}}^h(t) + \mathbf{A}\mathbf{u}^h(t) = \mathbf{b}^h(t), \qquad t \in J,$$
$$\mathbf{u}^h(0) = \mathbf{u}_0^h, \qquad (8.10)$$

Here, $\mathbf{A}$ is exactly the same stiffness matrix in (8.3). To discretize (8.10) in time, we employ the following simple forward time-stepping scheme.

$$\mathbf{u}_{n+1}^h = (\mathbf{I} - \Delta t \mathbf{A})\mathbf{u}_n^h + \Delta t \mathbf{b}_n^h,$$

for $n = 1, 2, \ldots, N_t - 1$ where $N_t \Delta t = T$, and $\mathbf{b}_n^h = \mathbf{b}^h(t_n)$.

8.4 Comparison of solutions of the classical and nonlocal heat equations

We compare the solutions of the nonlocal heat equation (8.9) to that of the classical heat equation

$$u_t(x, y, t) - \alpha \Delta u(x, y, t) = b(x, y, t), \quad (x, y, t) \in \Omega \times J,$$

equipped with the initial condition (8.9b) and the BC (8.5b). Here, α is a positive diffusivity parameter.

We employ the truncated series to approximate solutions of the classical heat Eq. 8.5a given in the form

$$u(x, y, t) = \sum_{m=1}^{M} \sum_{n=1}^{N} a_{mn} e^{-\alpha \frac{\pi^2}{4}(m^2+n^2)t} \sin\left(\frac{m\pi}{2}(x+1)\right) \sin\left(\frac{n\pi}{2}(y+1)\right)$$
(8.11)

where a_{mn} is given in (8.7) and the initial temperature $u_0(x, y)$ is given in (8.9b).

We depict the solutions of the classical and nonlocal wave equations at the cross section $y = 0$ for various t. The diffusivity parameter α is determined by requiring that the classical and nonlocal solutions coincide at $(x, y, t) = (0, 0, 0.01)$. For the continuous initial data, in Fig. 11 and we choose the horizon as $\delta = 2^{-3}$ and $\delta = 2^{-2}$ and set $\alpha = 0.059$ and $\alpha = 0.219$, respectively. We take

$$u_{0,\text{cont}}(x, y) = (x^2 - 1)(y^2 - 1). \tag{8.12}$$

The coefficients in (8.11) have the largest magnitude $|a_{mn}|$ at $t = 0$. For the initial data given in (8.12), we take $M = N = 11$, so that $|a_{MN}|e^{-\alpha \frac{\pi^2}{4}(m^2+n^2)t} \leq 10^{-6}$ for all $t \geq 0$.

For the discontinuous initial data, in Fig. 12 we choose the horizon as $\delta = 2^{-3}$ and $\delta = 2^{-2}$ and set $\alpha = 0.13$ and $\alpha = 0.24$, respectively. We take $u_{0,\text{disc}}(x, y) = u_{0,\text{disc}}(x)u_{0,\text{disc}}(y)$ where

$$u_{0,\text{disc}}(x) = \begin{cases} 1, & x \in [-1/2, 1/2], \\ 0, & \text{otherwise,} \end{cases} \tag{8.13}$$

For the initial data given in (8.13), we take $M = N = 33$, so that

$$|a_{MN}|e^{-\alpha \frac{\pi^2}{4}(m^2+n^2)t} \leq 10^{-6}, \quad \text{for all } t \geq 0.01.$$

In Fig. 11, with continuous initial data, we observe that the classical and nonlocal solutions are virtually identical for both values of δ. On the other hand, in Fig. 12, with discontinuous initial data, we also observe that the two solutions qualitatively agree for both values of δ in the sense that they both decay to the steady state solution
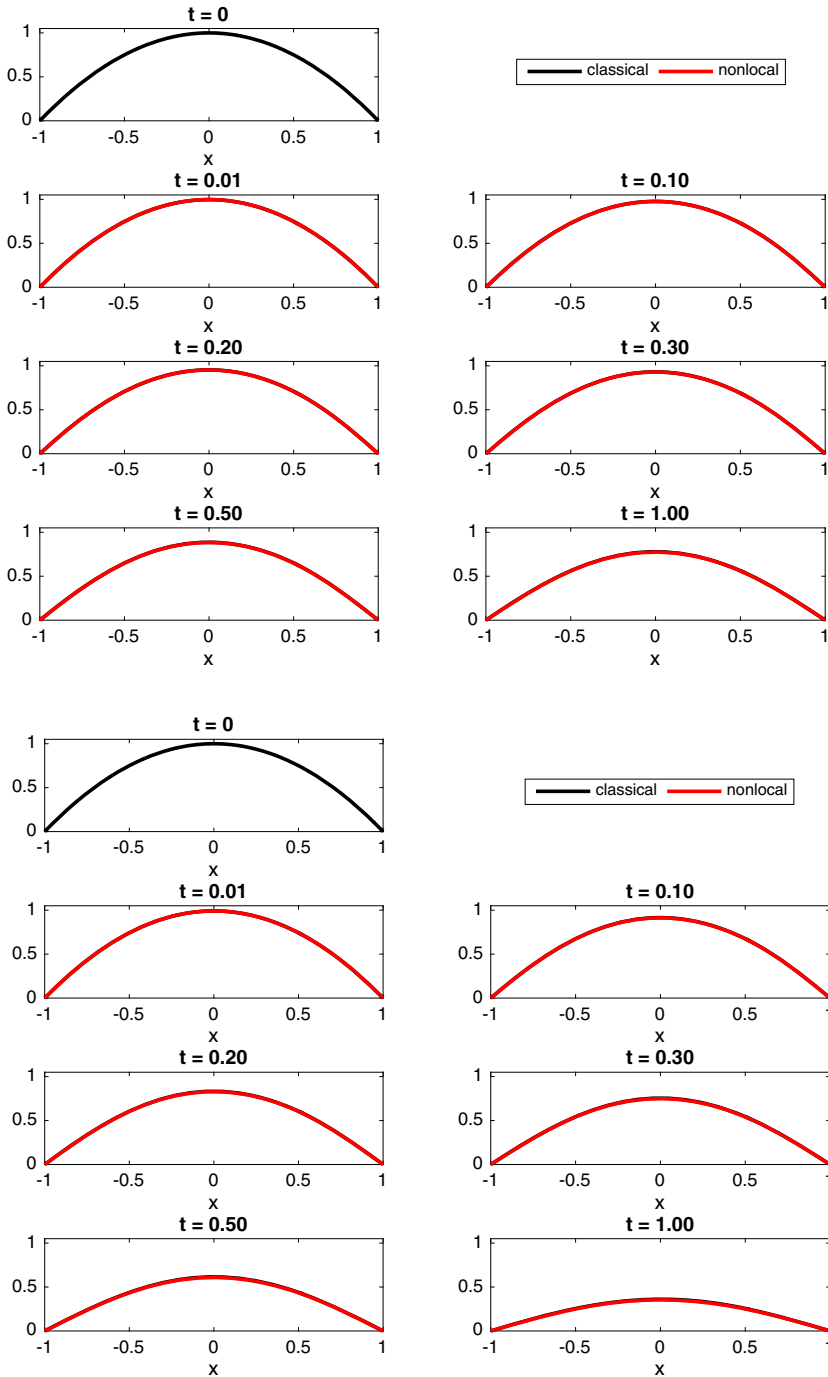
Fig. 11 Solutions $u(x, 0, t)$ to the 2D classical and nonlocal heat equations with continuous initial data. Top: $\delta = 2^{-3}$ and $\alpha = 0.059$. Bottom: $\delta = 2^{-2}$ and $\alpha = 0.219$
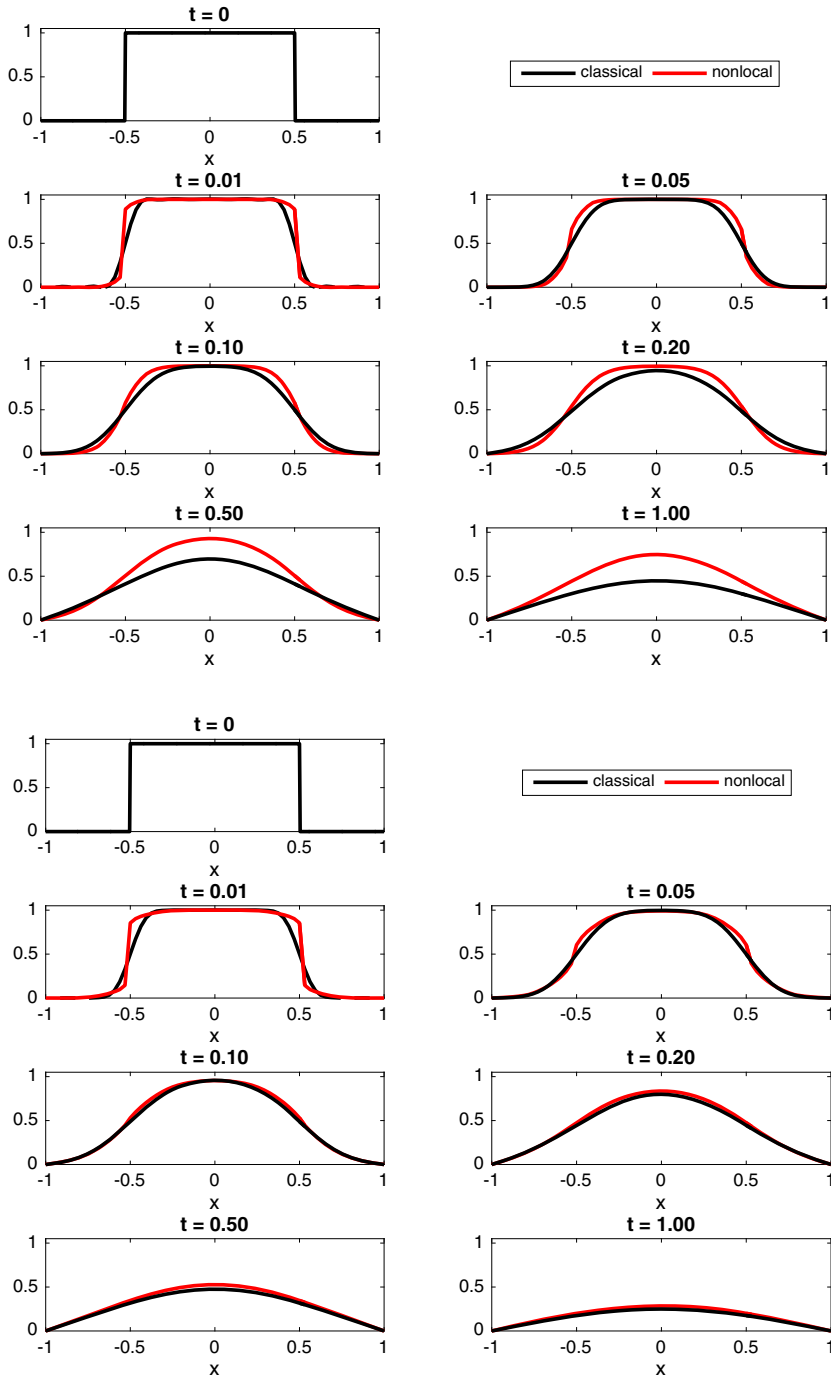
Fig. 12 Solutions $u(x, 0, t)$ to the 2D classical and nonlocal heat equations with discontinuous initial data. Top: $\delta = 2^{-3}$ and $\alpha = 0.13$. Bottom: $\delta = 2^{-2}$ and $\alpha = 0.24$

of $u = 0$. Yet, the agreement is more pronounced for large δ. In addition, both solutions follow a roughly similar profile at any given time. It is also worth noting that δ plays the role of the diffusivity parameter α. Namely, the larger the δ, the higher is the corresponding diffusivity.

9 Conclusion

We extended our recent work in 1D [4] to higher dimensions. We presented novel governing operators in 2D/3D for nonlocal wave propagation and nonlocal diffusion that enforce local BC. We presented methodically how to verify the BC by using a change in the order of integration. We provided 36 different types of BC in 2D which include pure and mixed combinations of Neumann, Dirichlet, periodic, and antiperiodic BC. We carried out numerical experiments for the nonlocal wave equation. We verified that the novel operators enforce local BC for all time. We also observed that the property we proved for 1D in [2], namely, discontinuities remain stationary, also holds for 2D. We provided a comparison of the solutions to the classical wave and heat equations to those of nonlocal ones. We found out that the classical and nonlocal wave propagation disagree, whereas, the classical and nonlocal diffusion agree.

Our ongoing work aims to extend these operators to vector valued problems which will help apply peridynamics to problems that require local BC. We anticipate that our novel approach will avoid altogether the surface effects seen in peridynamics. Our construction depends on the assumption of a rectangular/box geometry. We are investigating the case of general geometry in higher dimensions.

References

1. Aksoylu, B., Beyer, H.R., Celiker, F.: Application and implementation of incorporating local boundary conditions into nonlocal problems. Numer. Funct. Anal. Optim. **38**(9), 1077–1114 (2017). https://doi.org/10.1080/01630563.2017.1320674
2. Aksoylu, B., Beyer, H.R., Celiker, F.: Theoretical foundations of incorporating local boundary conditions into nonlocal problems. Rep. Math. Phys. **40**(1), 39–71 (2017). https://doi.org/10.1016/S0034-4877(17)30061-7
3. Aksoylu, B., Celiker, F.: Comparison of Nonlocal Operators Utilizing Perturbation Analysis. In: Others, B.K. (ed.) Numerical Mathematics and Advanced Applications ENUMATH 2015, Lecture Notes in Computational Science and Engineering, vol. 112, pp. 589–606. Springer (2016). https://doi.org/10.1007/978-3-319-39929-4_57
4. Aksoylu, B., Celiker, F.: Nonlocal problems with local Dirichlet and Neumann boundary conditions. J. Mech. Mater. Struct. **12**(4), 425–437 (2017). https://doi.org/10.2140/jomms.2017.12.425
5. Aksoylu, B., Celiker, F., Kilicer, O.: Nonlocal Problems with Local Boundary Conditions: An Overview. In: Voyiadjis, G.Z. (ed.) Handbook on Nonlocal Continuum Mechanics for Materials and Structures, pp. 1–38. Springer International Publishing, Cham (2018). https://doi.org/10.1007/978-3-319-22977-5_34-1

6. Aksoylu, B., Gazonas, G.A.: Inhomogeneous local boundary conditions in nonlocal problems. In: Proceedings of ECCOMAS2018, 6th European Conference on Computational Mechanics (ECCM 6) and 7th European Conference on Computational Fluid Dynamics (ECFD 7), 11-15. In press, Glasgow (2018)

7. Aksoylu, B., Gazonas, G.A.: On nonlocal problems with inhomogeneous local boundary conditions. Submitted

8. Aksoylu, B., Mengesha, T.: Results on nonlocal boundary value problems. Numer. Funct. Anal. Optim. **31**(12), 1301–1317 (2010). https://doi.org/10.1080/01630563.2010.519136

9. Aksoylu, B., Parks, M.L.: Variational theory and domain decomposition for nonlocal problems. Appl. Math. Comp. **217**, 6498–6515 (2011). https://doi.org/10.1016/j.amc.2011.01.027

10. Aksoylu, B., Unlu, Z.: Conditioning analysis of nonlocal integral operators in fractional Sobolev spaces. SIAM J. Numer. Anal. **52**(2), 653–677 (2014). https://doi.org/10.1137/13092407X

11. Andreu-Vaillo, F., Mazon, J.M., Rossi, J.D., Toledo-melero, J.: Nonlocal Diffusion problems, Mathematical Surveys and Monographs, vol. 165 American Mathematical Society and Real Socied Matematica Espanola (2010)

12. Beyer, H.R., Aksoylu, B., Celiker, F.: On a class of nonlocal wave equations from applications. J. Math. Phy. **57**(6), 062902 (2016). https://doi.org/10.1063/1.4953252. Eid: 062902

13. Bobaru, F., Duangpanya, M.: The peridynamic formulation for transient heat conduction. Int. J. Heat Mass Transf. **53**, 4047–4059 (2010)

14. Bobaru, F., Duangpanya, M.: A peridynamic formulation for transient heat conduction in bodies with evolving discontinuities. J. Comput. Phys. **231**, 2764–2785 (2012)

15. Caffarelli, L., Silvestre, L.: An extension problem related to the fractional Laplacian. Comm. Part. Diff. Eqs. **32**, 1245–1260 (2007)

16. Di Nezza, E., Palatucci, G., Valdinoci, E.: Hitchhiker's guide to fractional Sobolev spaces. Bull. Sci. Math. **136**(5), 521–573 (2012)

17. Du, Q., Gunzburger, M., Lehoucq, R.B., Zhou, K.: Analysis and approximation of nonlocal diffusion problems with volume constraints. SIAM Rev. **54**, 667–696 (2012)

18. Gilboa, G., Osher, S.: Nonlocal operators with applications to image processing. Multiscale Model Simul. **7**(3), 1005–1028 (2008)

19. Grote, M.J., Schneebeli, A., Schötzau, D.: Galerkin finite element method for the wave equation. SIAM J. Numer. Anal. **44**(6), 2408–2431 (2006)

20. Kamwal, R.P.: Linear Integral Equations: Theory and Technique. 2, Boston (1997)

21. Madenci, E., Oterkus, E.: Peridynamic Theory and Its Applications. Springer, New York (2014). https://doi.org/10.1007/978-1-4614-8465-3

22. Mitchell, J.A., Silling, S.A., Littlewood, D.J.: A position-aware linear solid constitutive model for peridynamics. J. Mech. Mater. Struct. **10**(5), 539–557 (2015)

23. Moiseiwistch, B.: Integral Equations. Longman Inc., New York (1977)

24. Nochetto, R.H., Otarola, E., Salgado, A.J.: a PDE approach to fractional diffusion in general domains: a priori error analysis. Found. Comput. Math. **15**, 733–791 (2015)

25. Oterkus, S., Madenci, E., Agwai, A.: Peridynamic thermal diffusion. J. Comput. Phys. **265**, 71–96 (2014)

26. Silling, S.: Reformulation of elasticity theory for discontinuities and long-range forces. J. Mech. Phys. Solids **48**, 175–209 (2000)

27. Tian, X., Du, Q.: Analysis and comparison of different approximations to nonlocal diffusion and linear peridynamic equations. SIAM J. Numer. Anal. **51**(6), 3458–3482 (2013)